Mechanism of S_N2 Alkylation Reactions of Lithium Organocuprate Clusters with Alkyl Halides and Epoxides. Solvent Effects, BF_3 Effects, and Trans-Diaxial Epoxide Opening

Seiji Mori,[§,‡] Eiichi Nakamura,*[,§] and Keiji Morokuma*[,‡]

Contribution from Department of Chemistry, The University of Tokyo, Bunkyo-ku, Tokyo 113-0033, Japan, and Cherry L. Emerson Center for Scientific Computation and Department of Chemistry, Emory University, Atlanta, Georgia 30322

Received January 19, 2000

Abstract: The B3LYP density functional studies on the mechanism of the S_N2-substitution reaction of methyl halides and epoxides with lithium organocuprates(I), $(CH_3)_2CuLi{\cdot}LiCl$ and $[(CH_3)_2CuLi]_2$, revealed the energetics and the geometries of important transition states and intermediates along the reaction pathway. In the absence of solvent coordination on the copper atom, the reaction takes place in a single step through rate determining cleavage of the C−X bond (X = leaving group) involving nucleophilic participation of the CH_3−Cu bond composed of the copper $3d_{z^2}$ orbital and carbon 2s+2p orbitals. Consideration of solvent polarity and coordination of an explicit $(CH_3)_2O$ molecule to a lithium atom in the cuprate cluster lowers the activation energy to <20 kcal/mol, which is a reasonable value for the reaction taking place below 0 °C. Solvation of the copper atom does not change much the geometry or the energy of the transition state, but modifies the pathway afterward. The origin of the "trans-diaxial opening of cyclohexene oxide" has been ascribed to the inverted stereochemistry of the electrophilic carbon atom in the rate-determining step of the reaction. Coordination of BF_3 lowers the activation energy of the nucleophilic ring opening of epoxide as much as to 9.2 kcal/mol. The origin of the acceleration of epoxide ring opening by BF_3 is attributed to the cooperative activation of borane and lithium atoms on the epoxide oxygen atom.

Introduction

The S_N2 substitution reaction of an organocopper(I) reagent with an alkyl halide and related electrophiles provides uniquely important synthetic methodology for C−C bond formation between a nonstabilized carbanion and a sp^3 electrophilic carbon center.[1] Organocopper(I) reagent is the oldest and still the only reagent of general utility for this transformation. In contrast to (anionic) cuprate(I) reagents that are reactive toward sp^3 electrophiles, neutral copper reagents such as RCu and RCu·PBu_3 are far less reactive.[2] Electrophiles such as alkyl halides, alkyl tosylates, epoxides, and azilidines[3] react smoothly with lithium diorganocuprate(I) reagents generally with inversion of stereochemistry at the electrophilic carbon atom (eq 1).[3,4] A more subtle stereochemical issue which has not received proper mechanistic attention is the regiochemistry of the ring opening of a cyclohexene oxide **1**. The reaction takes place with regiochemistry giving rise to a "trans-diaxial ring opening" product **3** rather than an alternative regioisomer **5** (eq 2).[5] In view of the apparently irreversible nature of the reaction, the regiochemistry must depend on the difference in the nature of the two transition states **2** and **4**, but no information on this issue has been available.

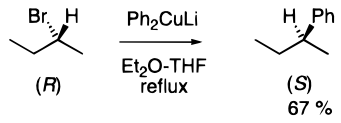

(1)

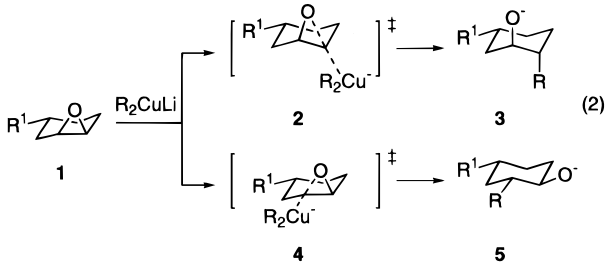

(2)

The alkylation reactions of R_2CuLi do not take place in the presence of a crown ether that generates solvent-separated R_2Cu^- species,[6,7] while the reaction of an epoxide is markedly

§ The University of Tokyo.

‡ Emory University.

(1) Reviews: Klunder, J. M.; Posner, G. H. In *Comprehensive Organic Synthesis*; Trost, B. M., Fleming, I. Eds.: Pergamon Press:: Elmsford, NY, 1991; Vol. 3, pp 207−239.

(2) (a) Herr, R. W.; Wieland, D. M.; Johnson, C. R. *J. Am. Chem. Soc.* **1970**, *92*, 3813−3814. (b) Johnson, C. R.; Herr, R. W.; Wieland, D. M. *J. Org. Chem.* **1973**, *38*, 4263−4268.

(3) Johnson, C. R.; Dutra, G. A. *J. Am. Chem. Soc.* **1973**, *95*, 7783−7787.

(4) Secondary iodides lose stereochemistry presumably through a single electron process. See: Lipshutz, B. H.; Wilhelm, R. S. *J. Am. Chem. Soc.* **1982**, *104*, 4696−4698. Ashby, E. C.; Coleman, D. *J. Org. Chem.* **1987**, *52*, 4554−4565. Bertz, S. H.; Dabbagh, G.; Mujsce, A. M. *J. Am. Chem. Soc.* **1991**, *113*, 631−636.

(5) Rickborn, B. In *Comprehensive Organic Synthesis*; Trost, B. M., Fleming, I., Eds.; Permagon Press: Elmsford, NY, 1991; Vol. 3, p 733.

(6) Ouannes, C.; Dressaire, G.; Langlois, Y. *Tetrahedron Lett.* **1977**, *10*, 815−818.

(7) The reaction of $(CH_3)_2CuLi{\cdot}LiI$ with 1-dodecanyl bromide did not take place (in Et_2O, 0 → 25 °C) in the presence of 12-crown-4 (see also ref 21b for similar effects in other classes of reactions). We thank A. Hirai for the experiments.

10.1021/ja0002060 CCC: $19.00
Published on Web 07/14/2000

accelerated in the presence of BF_3·Et_2O.[8,9] These data indicate that the nucleophilic organocopper reagent needs a certain Lewis acidic metal to be associated with the cuprate reagent, but the exact role of the Lewis acid remains uncertain.[10] One possibility is that the Lewis acid (LA) molecule coordinates with the electrofugal group as discussed in the case of the acid-catalyzed nucleophilic ring opening of an epoxide,[11] while another possibility involves the formation of a reagent composed of the cuprate and the Lewis acid prior to the reaction with the electrophile (eq 3).

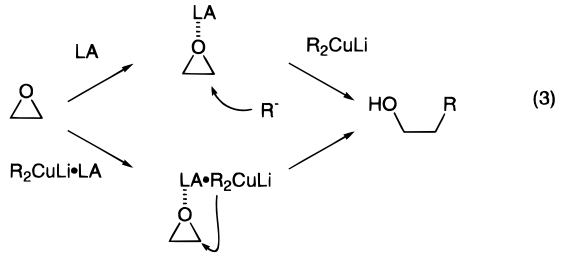

The reaction of R_2CuLi with an alkyl halide, an aryl halide, and an alkyl tosylate has been shown to be first order to the concentration of the R_2CuLi dimer and the alkylating reagent.[3,12,13,14] The magnitudes of primary and secondary kinetic isotope effects in the reaction of $(CH_3)_2CuLi$·LiI·PBu_3 with CH_3I are consistent with the rate determining bond breaking involving the electrophilic carbon center.[15]

Two mechanistic possibilities have been discussed for the reaction taking place with inversion of the electrophilic carbon atom: simple S_N2 reaction with the R anionic group (eq 4), and S_N2 reaction with the Cu atom (i.e., oxidative addition of R^1X to copper) followed by rapid reductive elimination of a trialkylcopper(III) intermediate (eq 5).[16] There has been neither

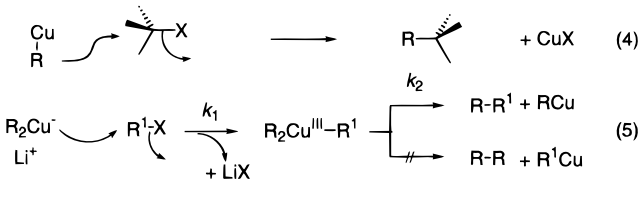

direct experimental evidence to differentiate these pathways nor theoretical analysis on the C−X displacement process (X = halide, O). Although the second mechanism appears to be reasonable, it left unanswered a few important questions; namely, the role of the lithium cation, the relative magnitude of k_1 and k_2, and, among others, the reason exclusive production of a cross-coupled product $R-R^1$ from the symmetrical $R_2(R^1)$-Cu(III) intermediate is always observed.[17,18] Despite the key roles of the Lewis acid (vide supra) and the lithium organocuprate cluster structure,[19,20] no discussion on their roles in the alkylation reactions has been made. With the density functional calculations, we have addressed these unsolved questions, and report the full details of the results obtained for the model reactions of cuprate clusters $(CH_3)_2CuLi$·$LiCl$ and $[(CH_3)_2CuLi]_2$ with electrophiles (CH_3Br, CH_3I, ethylene oxide, and cyclohexene oxide) with consideration of explicit solvent molecules, solvent polarity, and also a Lewis acid molecule (BF_3).[21,22]

Chemical Models

Methyl bromide, methyl iodide, ethylene oxide, and cyclohexene oxide were examined in the present studies since they are typical electrophiles in the S_N2 reaction of cuprates. The last substrate provided a chemical model most relevant to important synthetic problems of regio- and stereoselectivities of epoxide ring opening. Ethylene oxide was previously studied for the reaction with monomeric and dimeric methyllithium. [23]

Several aggregation states are known for lithium diorganocuprate-(I) species. Lithium diorganocuprate(I) reagents are usually prepared from an organolithium reagent and a copper(I) halide. These reagents exist as a dimeric aggregate (**A**) or as a species (**B**) of R_2CuLi·LiX stoichiometry (X = halide). Aggregation states may depend on solvent. For instance, R_2CuLi·LiI exists in ether as a dimer (**A**), whereas in THF it exists in R_2CuLi·LiI stoichiometry (**B**) as shown by molecular weight determination.[13,24] These stoichiometries are also supported by NMR[25,26] and EXAFS measurements.[13,20b] Crystals of several dimeric

(8) Dieter, R, K. In *Handbook of Reagents for Organic Synthesis, Reagents, Auxiliaries, and Catalysis for C−C Bond Formation*; Coates, R. M., Denmark, S. E., Eds.; John Wiley: Chichester, U.K., 1999; pp 457−458.

(9) (a) Ghribi, A.; Alexakis, A.; Normant, J. F. *Tetrahedron Lett.* **1984**, *25*, 3075−3078. Alexakis, A.; Jachiet, D.; Normant, J. F. *Tetrahedron*, **1986**, *42*, 5607−5619. (b) Eis, M. J.; Ganem, B. *Tetrahedron Lett.* **1985**, *26*, 1153−1156. Cf.: (c) Smith, A. B.; Jerris, P. J. *J. Am. Chem. Soc.* **1981**, *103*, 194−195.

(10) Cf.: Lipshutz, B. H.; Ellsworth, E. L.; Siahaan, T. J. *J. Am. Chem. Soc.* **1989**, *111*, 1351−1358.

(11) Yamamoto, Y.; Yamamoto, S.; Yatagai, H.; Maruyama, K. *J. Am. Chem. Soc.* **1980**, *102*, 2318−2325.

(12) Yamaguchi, M.; Hirao, I. *Tetrahedron Lett.* **1983**, *24*, 391−394.

(13) Pearson, R. G.; Gregory, C. D. *J. Am. Chem. Soc.* **1976**, *98*, 4098−4104. See also, ref 3.

(14) Spanenberg, W. J.; Snell, B. E.; Su, M.-C. *Microchem. J.* **1993**, *47*, 79−89.

(15) Guo, C.-y.; Brownawell, M. L.; San Filippo, J., Jr. *J. Am. Chem. Soc.* **1985**, *107*, 6028−6030.

(16) (a) Dorigo, A. E.; Wanner, J.; Schleyer, P. v. R. *Angew. Chem., Int. Ed. Engl.* **1995**, *34*, 476−478. (b) Snyder, J. P. *J. Am. Chem. Soc.* **1995**, *117*, 11025−11026.

(17) Komiya, S.; Albright, T. A.; Hoffmann, R.; Kochi, J. K. *J. Am. Chem. Soc.* **1976**, *98*, 7255−7265.

(18) Komiya, S.; Albright, T. A.; Hoffmann, R.; Kochi, J. K. *J. Am. Chem. Soc.* **1977**, *99*, 8440−8447.

(19) (a) Gerold, A.; Jastrzebski, J. T. B. H.; Kronenburg, C. M. P.; Krause, N.; van Koten, G. *Angew. Chem., Int. Ed. Engl.* **1997**, *36*, 755−757. (b) Snyder, J. P.; Tipsword, G. E.; Splanger, D. J. *J. Am. Chem. Soc.* **1992**, *114*, 1507−1510. Bertz, S. H.; Vellekoop, A. S.; Smith, R. A. J.; Snyder, J. P. *Organometallics* **1995**, *14*, 1213−1220.

(20) For pertinent references on cyanocuprates, see: (a) Snyder, J. P.; Splangler, D. P.; Behling, J. R.; Rossiter, B. E. *J. Org. Chem.* **1994**, *59*, 2665−2667. Snyder, J. P.; Bertz, S. H. *J. Org. Chem.* **1995**, *60*, 4312−4313. Huang, H.; Alvarez, K.; Cui, Q.; Barnhart, T. M.; Snyder, J. P.; Penner-Hahn J. E. *J. Am. Chem. Soc.* **1996**, *118*, 8808−8816; **1996**, *118*, 12252 (correction). Bertz, S. H.; Nilsson, K.; Davidson, Ö.; Snyder, J. P. *Angew. Chem., Int. Ed. Engl.* **1998**, *37*, 314−317. (b) Barnhart, T. M.; Huang, H.; Penner-Hahn, J. E. *J. Org. Chem.* **1995**, *60*, 4310−4311. (c) Stemmler, T. L.; Barnhart, T. M.; Penner-Hahn, J. E.; Tucker, C. E.; Knochel, P.; Böhme, M.; Frenking, G. *J. Am. Chem. Soc.* **1995**, *117*, 12489−12497. See also ref 19a for references.

(21) A preliminary report: Nakamura, E.; Mori, S.; Morokuma, K. *J. Am. Chem. Soc.* **1998**, *120*, 8273−8274 (3D pictures and coordinates are available on: http://WWW.chem.s.u-tokyo.ac.jp/∼common/Theo/Sn1/title).

(22) (a) Nakamura, E.; Mori, S.; Nakamura, M.; Morokuma, K. *J. Am. Chem. Soc.* **1997**, *119*, 4887−4899 (3D pictures and coordinates are available on: http://WWW.chem.s.u-tokyo.ac.jp/∼common/Theo/Cb/title). (b) Nakamura, E.; Mori, S.; Morokuma, K. *J. Am. Chem. Soc.* **1997**, *119*, 4900−4910 (3D pictures and coordinates are available on: http://WWW.chem.s.u-tokyo.ac.jp/∼common/Theo/Cj1/title). Mori, S.; Nakamura, E. *Chem. Eur. J.* **1999**, *5*, 1534−1543. (c) Mori, S.; Nakamura, E. *J. Mol. Struct (THEOCHEM)* **1999**, *461−462*, 167−175. (d) Mori, S.; Nakamura, E. *Tetrahedron Lett.* **1999**, *40*, 5319−5322. Mori, S.; Hirai, A.; Nakamura, M.; Nakamura, E. *Tetrahedron*, **2000**, 56, 2805−2809. (e) Nakamura, E.; Yamanaka, M. *J. Am. Chem. Soc.* **1999**, *121*, 8941−8942. (f) Nakamura, E.; Yamanaka, M.; Mori, S. *J. Am. Chem. Soc.* **2000**, *122*, 1826−1827.

(23) Harder, S.; van Lenthe, J. H.; van Eikema Hommes, N. J. R.; Schleyer, P. v. R. *J. Am. Chem. Soc.* **1994**, *116*, 2508−2514.

(24) van Koten, G.; Noltes, J. G. *J. Chem. Soc., Chem. Commun.* **1972**, 940−941.

(25) Bertz, S. H.; Vellekoop, A. S.; Smith, R. A. J.; Snyder, J. P. *Organometallics* **1995**, *14*, 1213−1220.

(26) (a) Ashby, E. C.; Watkins, J. J. *J. Am. Chem. Soc.* **1977**, *99*, 5312−5317. (b) van Koten, G.; Noltes, J. G. *J. Organomet. Chem.* **1979**, *174*, 367−387. (c) Lipshutz, B. H.; Kozlowski, J. A.; Breneman, C. M. *J. Am. Chem. Soc.* **1985**, *107*, 3197−3204.

cuprate(I) complexes were determined by X-ray crystallographic analysis.[27] The R−Li bond is electrostatic in nature, and may readily dissociate in a polar medium (i.e., THF).[28] In the presence of a stronger Lewis base such as a crown ether, an ion-pair of the cuprate such as **C** is formed as examined by X-ray crystallographic analyses.[29] **C** is, however, not a reactive nucleophile.[6,7,22a]

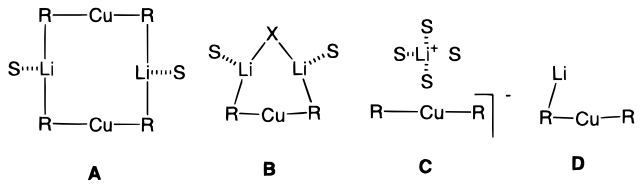

S = solvent, X = Cl, Br, I, CN

We previously examined the reaction of acetylene with various model organocopper(I) compounds, CH_3Cu, $(CH_3)_2Cu^-$, $(CH_3)_2CuLi$ (**D**, R = CH_3), $(CH_3)_2CuLi{\cdot}LiCl$ (**B**, R = CH_3, X = Cl; S = none), and $[(CH_3)_2CuLi]_2$ (**A**, S = none), by ab initio and density functional methods.[22] CH_3Cu itself is very nucleophilic due to its lacking 3d orbitals.[22c] Dimethylcuprate(I) anion (R_2Cu^-, **C**) is more nucleophilic than CH_3Cu, but both experimental and theoretical studies on its reactivities toward acetylene showed that it is not as reactive as **A** or **B**. We found that both $[(CH_3)_2CuLi]_2$ (**A**) and $(CH_3)_2CuLi.LiX$ (**B**) can be equally responsible as the reactive species in the nucleophilic chemistry of organocuprates.[22a]

In the organocuprate reactions, solvent coordination is also important, and therefore we examined dimethyl ether and dimethyl sulfide molecules as models of explicit solvent models. The latter is sometimes contained in cuprate reagents which are frequently used as a Cu(I) source.[30,31] In the studies on MeBr and CH_3I, we examined $(CH_3)_2O$, and in those on epoxide, we examined both $(CH_3)_2O$ and $(CH_3)_2S$. We found that the results with $(CH_3)_2O$ and $(CH_3)_2S$ are essentially the same, only they show the $(CH_3)_2S$ results.

To examine the effects of Lewis acid on the alkylation of epoxides, we examined the coordination of BF_3 on ethylene oxide in the reaction with $(CH_3)_2CuLi{\cdot}LiCl{\cdot}(CH_3)_2O$.

Computational Methods

Theoretical calculations were performed on a Gaussian 98 program package[32] with the B3LYP hybrid functional[33] with the basis sets denoted as B3LYP/631A, which consisted of the Ahlrichs all-electron SVP basis sets[34] for Cu and Br atoms, quasi-relativistic effective-core potential (ECP) for an iodine atom,[35] and 6-31G(d)[36] for the rest. To prove the relativistic effects on Cu, quasi-relativistic ECP[31] for Cu was examined for the transition state of the reaction of methyl iodide with $(CH_3)_2CuLi{\cdot}LiCl{\cdot}(CH_3)_2O$ to find that the relativistic effects are small (data not shown; relativistic effects were also found to be small for the carbocupration of acetylene).[22a] The B3LYP/631A method gave qualitatively the same structures as those obtained at the MP2(FC) level of theory[22a,37] and the B3LYP energies were in reasonable agreement with the CCSD(T)/B3LYP values.[22a] Stationary points were optimized without any symmetry assumption unless noted otherwise. One imaginary frequency for all transition structures (TSs) was confirmed by normal coordinate analysis. Zero-point energies and entropies of some stationary points were evaluated based on harmonic frequencies. Natural charges[38] were calculated at the same level as the level for geometry optimizations. For the intrinsic reaction coordinate (IRC) analysis,[39] we used the B3LYP/631A level of theory.

The Boys localization procedure[40] was performed to obtain localized MOs from the occupied B3LYP/631A Kohn−Sham MOs[41] for the B3LYP/631A geometries. Contour maps of molecular orbitals were displayed using Molden 3.2.[42]

Evaluation of the effects of solvent polarity was carried out for one reaction pathway involving **IVc** and **TS-VIc** with the aid of two theoretical methods. The self-consistent reaction field (SCRF) method based on the Onsager model (ϵ = 4.34 for Et_2O, 20 °C[43])[44] was performed with full geometry optimization of these structures, and we found that the geometries remained largely the same as those in the gas phase (data not shown). Atomic radii were estimated by Monte Carlo integration, within a selected density contour (0.001 electron/bohr^3),[45] implemented in Gaussian 98. Recommended molecular radii (a_0) of **IVc** and **TS-VIc** are 4.97 and 4.91 Å, respectively. We also performed single point energy calculations of the polarized continuum model (PCM) method[46] at the gas-phase geometries and found that activation energy decreases considerably (vide infra). Atomic radii were used by default (UAHF radii for C,O, S, and Br, and UFF radii for other atoms).

Kinetic isotope effects[47] were computed, as reported previously for cuprate conjugate addition,[22b] by the Bigeleisen−Mayer's equation[48] with Wigner tunnel correction based on the calculated frequencies scaled

(27) (a) van Koten, G.; Jastrzebski, J. T. B. H.; Muller, F.; Stam, C. H. *J. Am. Chem. Soc.* **1985**, *107*, 697−698. (b) Lorenzen, N. P.; Weiss, E. *Angew. Chem., Int. Ed. Engl.* **1990**, *29*, 300−302. (c) Olmstead, M. M.; Power, P. P. *Organometallics* **1990**, *9*, 1720−1722. (d) Olmstead, M. M.; Power, P. P. *J. Am. Chem. Soc.* **1990**, *112*, 8008−8014.

(28) Mobley, T. A.; Müller, F.; Berger, S. *J. Am. Chem. Soc.* **1998**, *120*, 1333−1334.

(29) Hope, H.; Olmstead, M. M.; Power, P. P.; Sandell, J.; Xu, X. *J. Am. Chem. Soc.* **1985**, *107*, 4337−4338.

(30) (a) House, H. O.; Chu, C.-Y.; Wilkins, J. M.; Umen, M. J. *J. Org. Chem.* **1975**, *10*, 1460−1469. (b) Westmijze, H.; Kleijn, H.; Vermeer, P.; *Tetrahedron Lett.* **1977**, *23*, 2023−2026. (c) Bertz, S. H.; Fairchild, E. H. In *Encyclopedia of Reagents for Organic Synthesis;* Paquette, L. A., Ed.; John Wiley: Chichester, U.K., 1995; Vol. 2, pp 1312−1315.

(31) Bertz, S. H.; Dabbagh, G. *J. Org. Chem.* **1984**, *49*, 1119−1122. Bertz, S. H. *J. Am. Chem. Soc.* **1990**, *112*, 4031−4032. Bertz, S. H.; Fairchild, E. H. In *Encyclopedia of Reagents for Organic Synthesis;* Paquette, L. A., Ed.; John Wiley: Chichester, 1995; Vol. 2, pp 1346−1349.

(32) Gaussian 98, Revision A.6, Frisch, M. J.; Trucks, G. W.; Schlegel, H. B.; Scuseria, G. E.; Robb, M. A.; Cheeseman, J. R.; Zakrzewski, V. G.; Montgomery, J. A., Jr.; Stratmann, R. E.; Burant, J. C.; Dapprich, S.; Millam, J. M.; Daniels, A. D.; Kudin, K. N.; Strain, M. C.; Farkas, O.; Tomasi, J.; Barone, V.; Cossi, M.; Cammi, R.; Mennucci, B.; Pomelli, C.; Adamo, C.; Clifford, S.; Ochterski, J.; Petersson, G. A.; Ayala, P. Y.; Cui, Q.; Morokuma, K.; Malick, D. K.; Rabuck, A. D.; Raghavachari, K.; Foresman, J. B.; Cioslowski, J.; Ortiz, J. V.; Stefanov, B. B.; Liu, G.; Liashenko, A.; Piskorz, P.; Komaromi, I.; Gomperts, R.; Martin, R. L.; Fox, D. J.; Keith, T.; Al-Laham, M. A.; Peng, C. Y.; Nanayakkara, A.; Gonzalez, C.; Challacombe, M.; Gill, P. M. W.; Johnson, B.; Chen, W.; Wong, M. W.; Andres, J. L.; Head-Gordon, M.; Replogle, E. S.; Pople, J. A. Gaussian Inc.: Pittsburgh, PA, 1998.

(33) Becke, A. D. *J. Chem. Phys.* **1993**, *98*, 5648−5652. Lee, C.; Yang, W.; Parr, R. G. *Phys. Rev. B* **1988**, *37*, 785−789.

(34) Schäfer, A.; Horn, H.; Ahlrichs, R. *J. Chem. Phys.* **1992**, 97, 2571−2577.

(35) Bergner, A.; Dolg, M.; Kuechle, W.; Stoll, H.; Preuss, H. *Mol. Phys.* **1993**, *80*, 1431−1441.

(36) Hehre, W. J.; Radom, L.; Schleyer, P. v. R.; Pople, J. A. *Ab Initio Molecular Orbital Theory*; John Wiley: New York, 1986. References cited therein.

(37) MP2(FC) (FC = frozen core): Møller, C.; Plesset, M. S. *Phys. Rev.* **1934**, *46*, 618−622. Pople, J. A.; Krishman, R.; Schlegel, H. B.; Binkley, J. S. *Int. J. Quantum. Chem. Symp.* **1979**, *13*, 225−241.

(38) Reed, A. E.; Curtiss, L. A.; Weinhold, F. *Chem. Rev.* **1988**, *88*, 899−926. NBO Version 3.1 in the Gaussian 98 package implemented by Glendening, E. D.; Reed, A. E.; Carpenter, J. E.; Weinhold, F.; University of Wisconsin: Madison, WI, 1990.

(39) Fukui, K. *Acc. Chem. Res.* **1981**, *14*, 363−368. Gonzalez, C.; Schlegel, H. B. *J. Chem. Phys.* **1989**, *90*, 2154−2161. Gonzalez, C.; Schlegel, H. B. *J. Phys. Chem.* **1990**, *94*, 5523−5527.

(40) Boys, S. F. *Quantum Theory of Atoms, Molecules, and the Solid State*; Lowdin, P. O., Ed.; Academic Press: New York, 1968; pp 253−262. Haddon, R. C.; Williams, G. R. J. *Chem. Phys. Lett.* **1976**, *42*, 453−455.

(41) Kohn, W.; Sham, L. J. *Phys. Rev.* **1965**, *140*, A1133−A1138.

(42) Schaftenaar, G. Molden 3.2, University of Nijmegen, Nijmegen, The Netherlands 1997.

(43) *CRC Handbook of Chemistry and Physics*; Lide, D. R., Ed.; CRC Press: Boca Raton, FL, 1992; pp 9-52 to 9-53.

(44) See: Onsager, L. *J. Am. Chem. Soc.* **1936**, *58*, 1486−1493. Tapia, O.; Goscinski, O. *Mol. Phys.* **1975**, *29*, 1653−1661. Wong, M. W.; Wiberg, K. B.; Frisch, M. *J. Chem. Phys.* **1991**, *95*, 8991−8998. Wong, M. W.; Wiberg, K. B.; Frisch, M. J. *J. Comput. Chem.* **1995**, *16*, 385−394.

(45) Wong, M. W.; Wiberg, K. B.; Frisch, M. J. *J. Comput. Chem.* **1995**, *16*, 386−394.

(46) Miertus, S.; Scrocco, E.; Tomasi, J. *Chem. Phys.* **1981**, *55*, 117−129. Miertus, S.; Tomasi, J. *Chem. Phys.* **1982**, *65*, 239−245. Barone, V.; Cossi, M.; Tomasi, J. *J. Comput. Chem.* **1998**, *19*, 404−417.

Scheme 1. Substitution Reaction between $(CH_3)_2CuLi\cdot LiCl$ and CH_3Br with and without $(CH_3)_2O$[a]

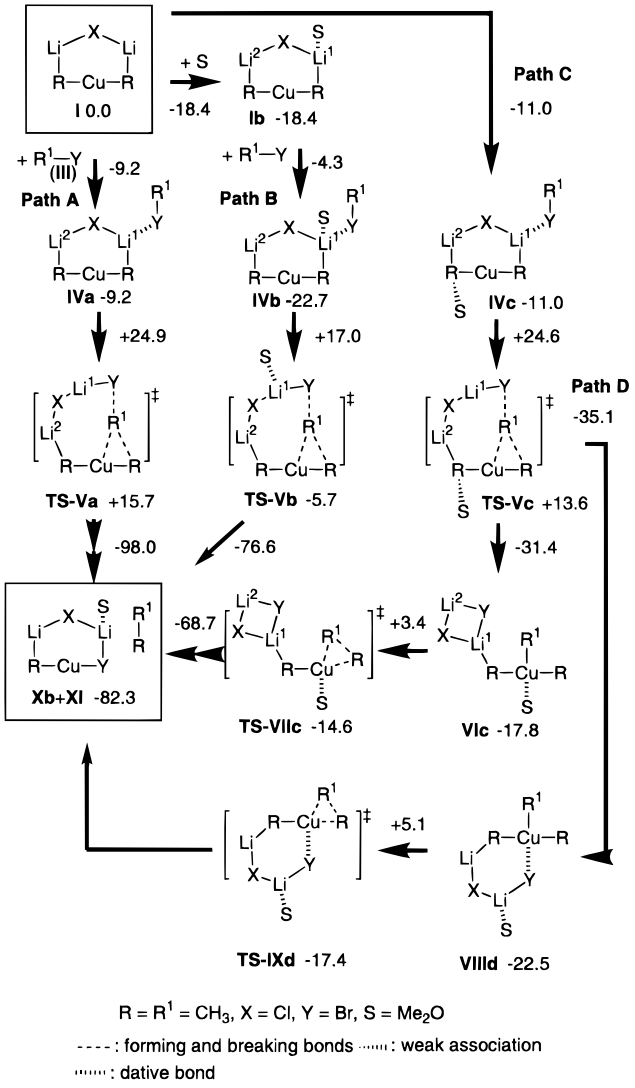

[a] The energy change on each shown on a side of an arrow is in kcal/mol. The structures in path N (N = A, B, C, and D) are numbered in roman numerals followed by n to Identify the path (n = a, b, c, and d, respectively). Note that the final product mixture in the box is rather formal, and may be less stable than the reality, which must be various aggregated or polymeric species.

by 0.9614 at the B3LYP/631A level,[49] respectively. The original Bigeleisen−Mayer's equation without tunnel effect consideration was also used to evaluate the tunneling effect. By inclusion of the tunneling effect, the largest deviation of KIEs was found to be +0.010, which was found to be in the H/D KIE of **TS-VIIc** where CH_3Br (**II**) was taken as a starting reference material**.** There have been reported several studies that the theoretical KIEs obtained by B3LYP methods are in good agreement with the experimental KIEs.[50]

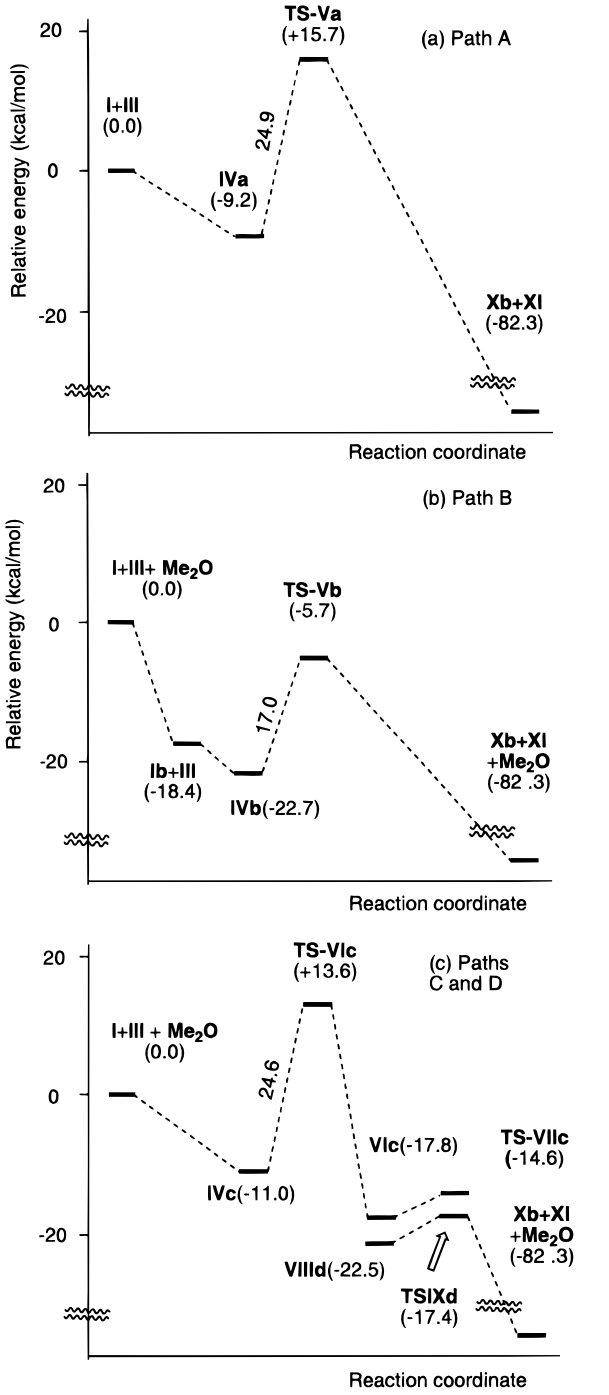

Figure 1. Energy changes of the CH_3Br reaction in (a) path A, (b) path B, and (c) paths C and D at the B3LYP/631A level. Values in parentheses are energies relative to the reactants in kcal/mol.

Results and Discussions

1. S_N2 Reaction with CH_3Br. The S_N2 reaction of alkyl bromides takes place with inversion of the stereochemistry, and is modeled by the reaction of **I** ($(CH_3)_2CuLi\cdot LiCl$) and **II** ($[(CH_3)_2CuLi]_2$) with methyl bromide(**III**, CH_3Br) in the presence and absence of a coordinating solvent molecule ($(CH_3)_2O$ or $(CH_3)_2S$). In the unsolvated pathway (path A in Scheme 1) and Figure 2, coordination of CH_3Br with the Li^1 atom of **I** generates, with 9.2 kcal/mol (Figure 1a) stabilization energy, a complex (**IVa**, Figure 2) in which the C^b-Li^1 bond is elongated by 2% and the C^a-Cu bond slightly shortened. In the complex **IVa**, a bromine atom is almost neutral (−0.043). Further elongation of the C^a-Li^1 bond leads to the transition structure

(47) Melander, L.; W. H. Saunders, W. H. *Reaction Rates of Isotopic Molecules*; Wiley: Chichester, 1980.
(48) Bigeleisen, J.; Mayer, M. G. *J. Chem. Phys.* **1947**, *15*, 261−267. Bigeleisen, J.; Wolfsberg, M. *Adv. Chem. Phys.* **1958**, *1*, 15−76. See also: Yamataka, H.; Nagase, S. *J. Am. Chem. Soc.* **1998**, *120*, 7530−7536.
(49) Scott, A. P.; Radom, L. *J. Phys. Chem.* **1996**, *100*, 16502−16513
(50) Examples: DelMonte, A. J.; Haller, J.; Houk, K. N.; Sharpless, K. B.; Singleton, D. A.; Strassner, T.; Thomas, A. A. *J. Am. Chem. Soc.* **1997**, *119*, 9907−9908. Keating, A. E.; Merrigan, S. R.; Singleton, D. A.; Houk, K. N. *J. Am. Chem. Soc.* **1999**, *121*, 3933−3938. Frantz, D. E.; Singleton, D. A.; Snyder, J. P. *J. Am. Chem. Soc.* **1997**, *119*, 3383−3384. Frantz, D. E.; Singleton, D. A. *J. Am. Chem. Soc.* **2000**, *122*, 3288−3295. Cf.: Czyryca, P.; Paneth, P. *J. Org. Chem.* **1997**, *62*, 7305−7309.

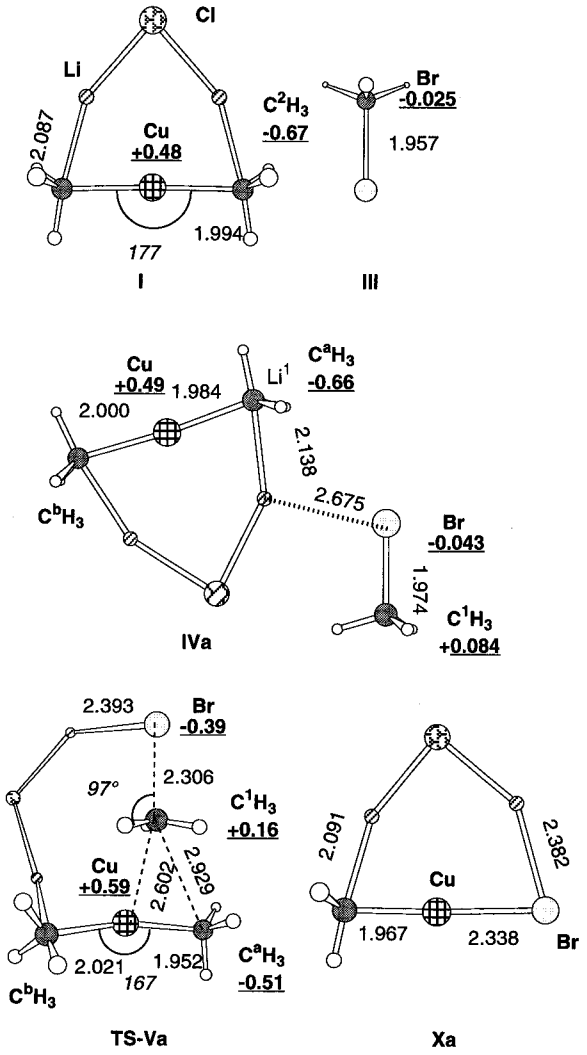

Figure 2. (a) 3D representations of stationary points in the reaction of $(CH_3)_2CuLi{\cdot}LiCl$ with CH_3Br at the $B_3LYP/631A$ level. Shown are bond lengths in Å, bond angles (in italic) in deg, and natural charge (in underlined bold). The value of an imaginary frequency in **TS-Va** is 218.0*i* cm^{-1}.

(TS) of C¹−Br bond cleavage (**TS**−**Va**) with an activation energy of 24.9 kcal/mol. In **TS-Va**, the C¹−Br bond is elongated only by 17% relative to **IVa**, and the stereochemistry of the electrophilic carbon of CH_3Br is not inverted yet (note that the stereochemistry of the electrophilic center in the epoxide reaction (vide infra) is inverted). The Br atom is negatively charged (−0.39). In **TS-Va**, the Li¹−Br distance of 2.393 Å is shorter than that in **IVa**. Structural feature of **TS-Va** (and all other TSs of the displacement step discussed in this paper) is that the Cᵃ−Cu cuprate moiety largely retains its original geometry, the Cᵃ−Cu bond being still short and the Cᵃ−Cu−Cᵇ angle nearly linear. One can identify an open cluster structure[22a,b] in **TS-Va**, which enables the operation of a push−pull activation of the halide. IRC (intrinsic reaction coordinate) following back from **TS-Va** to the point of $s = -4.81$ $amu^{1/2}{\cdot}bohr$ and subsequent optimization led monotonically downhill to the closed cluster **IVa**. IRC following the forward direction (data not shown) goes through an intermediary (nonstationary) structure similar to **VIc** (vide infra) and smoothly downhill toward ethane (**XI**) and CH_3-Br·LiBr·LiCl (a structure the same as **Xb** but lacking the solvent molecule).

We also examine (Figure 3) the lithium/bromide complex **XIIa** and the bromide displacement TS (**TS-XIIIa**) for the

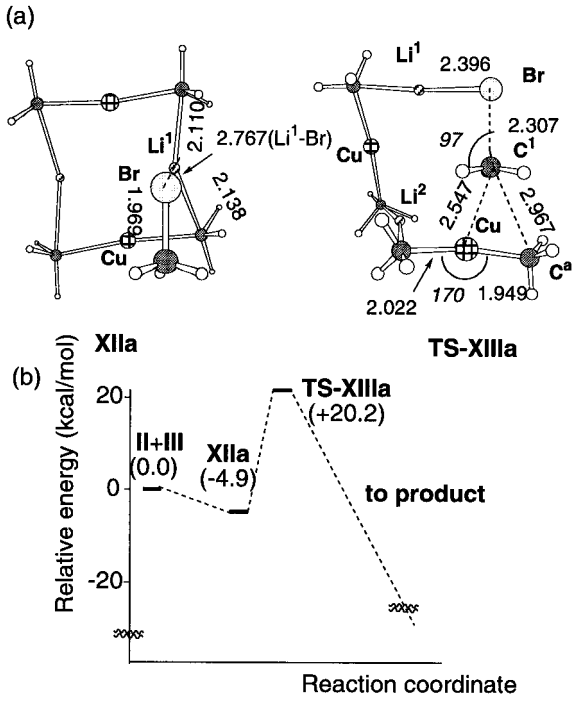

Figure 3. (a) 3D representations and (b) energetics in the reaction of $[(CH_3)_2CuLi]_2$ (**II**) with CH_3Br (**III**) at the B3LYP/631A level. See Figure 2 for details. The value of an imaginary frequency in **TS-XIIIa** is 224.0*i* cm^{-1}.

dimeric lithium dimethylcuprate(I) [**II**, $(CH_3)_2CuLi]_2$. **TS-XIIIa** is essentially the same as **TS-Va** as to the $C^2H_3-Cu-C^1H_3-Br-Li$ moiety.

Effects of solvent coordination are examined next (paths B and C in Scheme 1). Coordination of a molecule of solvent $(CH_3)_2O$ to Li¹ (path B, Figure 1b and 4) elongated the Li¹−Br distance (12% from **IVa** to **IVb** and 2.5% from **TS-Va** to **TS**−**Vb**) and this coordination does not much change the geometry of the TS (**IVb** and **TSVb** in Figure 4) but lowers the activation energy of the bromide displacement process (path B) by 7.9 to 17.0 kcal/mol.[51] Coordination to both Li¹ and Li² did not change much the geometry of the transition state (**TS-XIVb** vs **TS-Vb**, Figure 4). When solvent polarity was considered at the B3LYP(PCM, solvent = THF)/631A//B3LYP/631A level for path A (i.e. without explicit solvent), the activation energy decreased from 24.9 to 16.9 kcal/mol. Effects of zero-point energies (ZPE) and entropies are also small ($\Delta ZPE = -1.0$ kcal/mol, $\Delta\Delta S^{\ddagger} = -0.33$ cal/(mol·K) at 298.15 K). Taken together, these data suggest that the actual reaction in ether may be estimated to be well below 20 kcal/mol, which is a reasonable value for the reaction taking place below ca. 0 °C.

While solvent coordination on Cu (path C in Scheme 1, Figures 1 and 5) has only small effects on the energetics and the structures up to the rate-determining C−Br bond cleaving step, this substantially modifies the pathway afterwards. For instance, before the TS of C−Br bond cleavage, we found no sign of strong solvent−Cu(I) coordination because the copper-(I) atom already bears two CH_3^- groups.[52] Structures of **IVc**

(51) For solvent coordination numbers vs energetics, see: Rodgers, M. T.; Armentrout, P. B. *J. Phys. Chem. A* **1997**, *101*, 1238−1249.

(52) The copper atom in lithium organocuprate does not accept any neutral ligand on copper as confirmed by lack of such structures in the Cambridge Crystallographic Database (version 2.3.7, 1998). See also: Power, P. P. *Prog. Inorg. Chem.* **1991**, *39*, 75−112. In dimethyl sulfide solution, there is no evidence for Cu−S coordination. See: Huang, H.; Liang, C. H.; Penner-Hahn, J. E. *Angew. Chem., Int. Ed. Engl.* **1998**, *37*, 1564−1566.

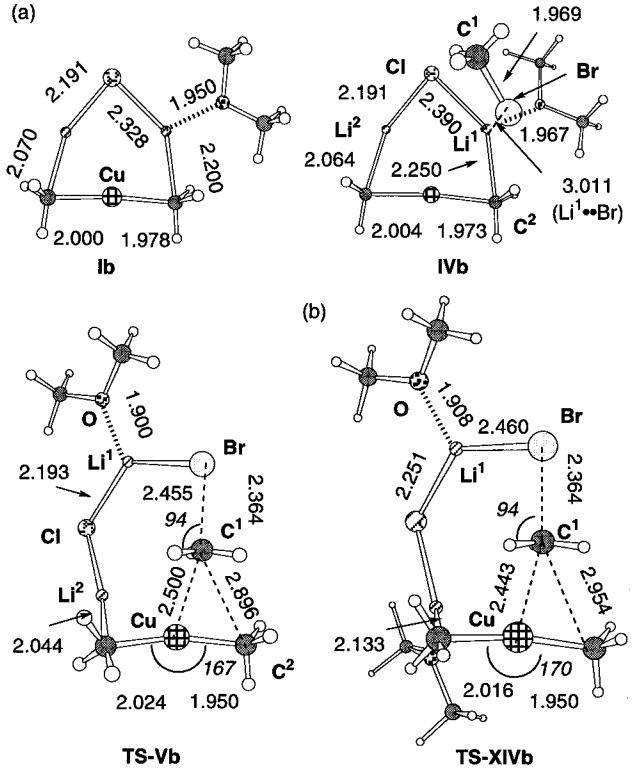

Figure 4. (a) 3D structures and (b) energy changes of **Ib**, **IVb**, and **TS-Vb** in the $(CH_3)_2CuLi{\cdot}LiCl{\cdot}(CH_3)_2O$ reaction and (b) TS (**TS-XIVb**) in the $(CH_3)_2CuLi{\cdot}LiCl{\cdot}2(CH_3)_2O$ reaction at the B3LYP/631A level. See also Scheme 1. The values of imaginary frequencies for **TS-Vb** and **TS-XIVb** are 259.8*i* and 243.9*i* cm^{-1}, respectively.

and **TS-Vc** (in path C and Figure 5) are not true copper-solvated species, but weak association complexes ($Cu{\cdot\cdot}HCH_2OCH_3$, ca. 3 Å, $Cu{\cdot\cdot}O$ = ca. 4 Å). Such a weak association of an ether molecule little affected the activation energy ($\Delta E^{\ddagger} = 24.6$ kcal/mol, $\Delta S^{\ddagger} = -3.97$ cal/(mol·K) at 298.15 K, $\Delta G^{\ddagger} = 24.6$ kcal/mol at 298.15 K).

Stronger solvent coordination to Cu occurs, however, after negative charge is transferred from the cuprate to the CH_3Br moiety. Thus, a kinetically unstable $(CH_3)_3Cu(III)$ intermediate (**VIc**)[16] is located as a minimum, which gives ethane with only 3.4 kcal/mol activation energy via **TS-VIIc** (Figures 1c and 5). $(CH_3)_3Cu[(CH_3)_2O]$ without the Lewis acidic LiBr·LiCl cluster undergoes reductive elimination with a much higher activation energy of 8.2 kcal/mol (B3LYP/631A). Notably, the KIEs calculated for the decomposition of **VIc** via **TS-VIIc** are far from the experimental data (vide supra). Thus, **TS-VIIc** does not comprise the rate determining stage of the S_N2 reaction, and hence **VIc** is not a kinetically important species.

We also considered another possibility (path D) of ligand coordination to a Cu(III) intermediate, namely, when we put the dissociating bromine atom on the copper atom. We obtained an alternative intermediate, **VIIId**, with a planar four-coordinate geometry.[22f] This was located 4.8 kcal/mol lower in energy than **VIc**, and the reductive elimination occurs with the activation barrier of 5.1 kcal/mol via **TS-IXd**. Zero-point energies and entropies do not affect the energy difference between paths C and D very much. **TS-IXd** is still lower in Gibbs free energy than **TS-VIIc** ($\Delta\Delta G^{\ddagger} = 3.0$ kcal/mol at 298.15 K). Therefore, path D could be favorable over path C in solution.

In paths A−C (cf. **TS-Va**, **TS-Vb**, and **TS-Vc**) the stereochemistry at the electrophilic and the nucleophilic carbon centers is inversion and retention, respectively. Since the reductive

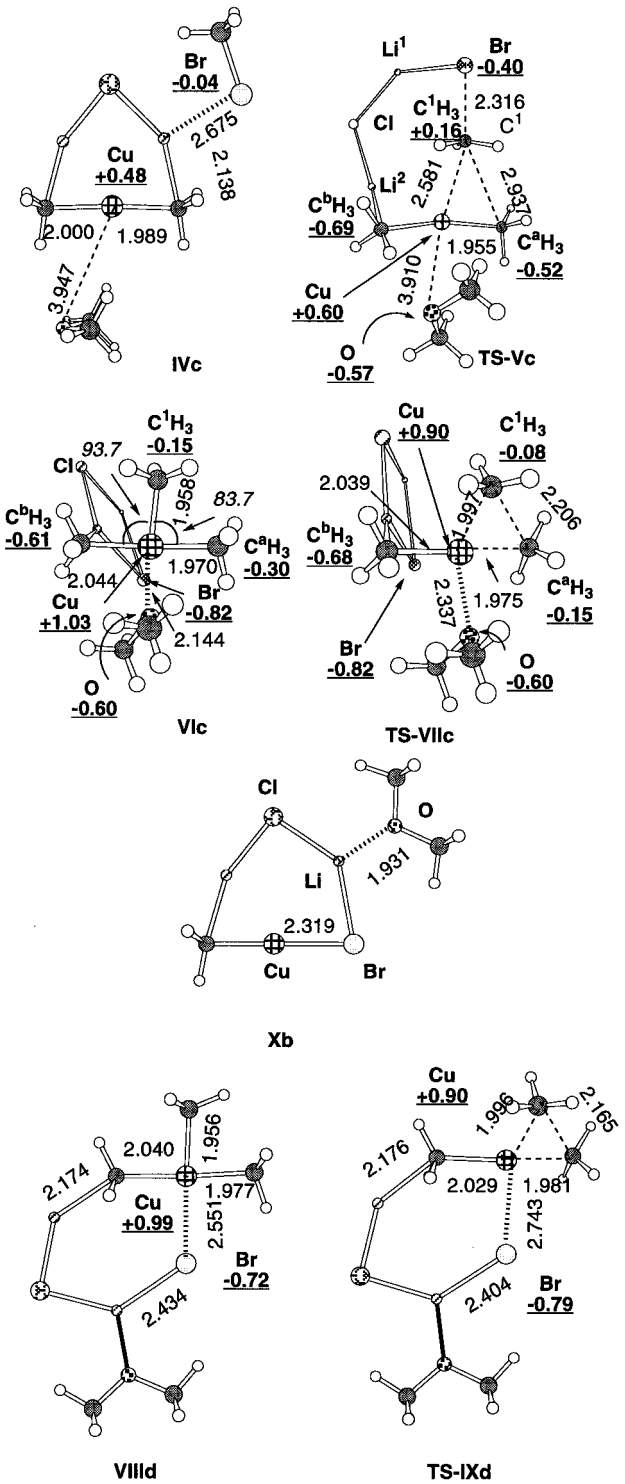

Figure 5. B3LYP stationary points in the reaction of $(CH_3)_2CuLi{\cdot}LiCl{\cdot}(CH_3)_2O$ with CH_3Br. See also Scheme 1. The values of imaginary frequencies for **TS-Vc**, **TS-VIIc**, and **TS-IXd** are 226.4*i*, 271.9*i*, and 302.1*i* cm^{-1}, respectively.

elimination of **VIc** and **VIIId** (Scheme 1) also proceeds with retention (cf. **TS-VIIc** and **TS-IXd**), the net results of the S_N2 reaction through all paths A−D will be inversion at the electrophilic carbon center and retention at the nucleophilic carbon center.

It is important to note that the group selectivity issue (eq 2) does not arise in paths A and B, or even in paths C and D, where three methyl groups are in different electronic and spatial environment.

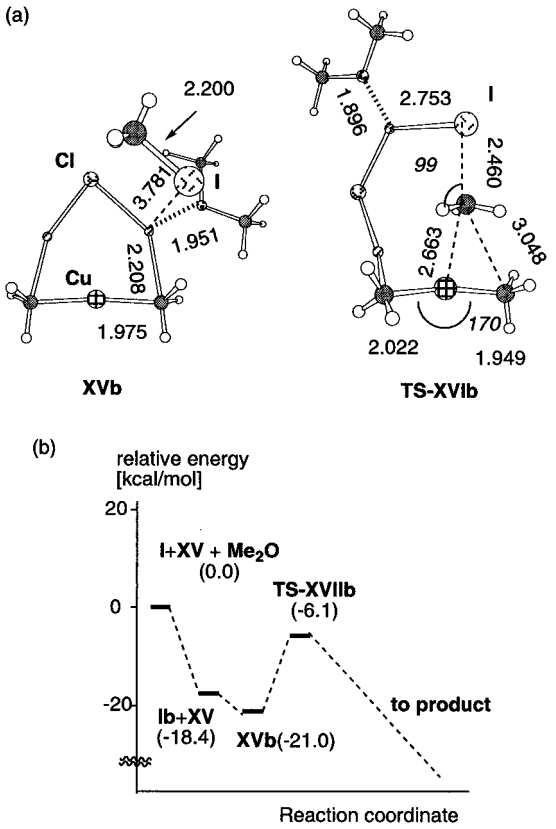

Figure 6. (a) 3D structures of **XVIb** and **TS-XVIIb** at the B3LYP/631A level. The value of an imaginary frequency for **TS-XVIIb** is 116.6*i* cm^{-1}. (b) Energetics of the reaction with CH_3I.

2. S_N2 Reaction with CH_3I. Methyl iodide was examined next. The studies on kinetic isotope effects were previously reported (vide infra), and showed that the iodide displacement step is the rate determining step of the reaction. The reaction of $(CH_3)_2CuLi{\cdot}LiCl{\cdot}(CH_3)_2O$ with CH_3I (**XV**) (Figure 6 and path B in Scheme 1) was examined to locate the complex **XVIb** and TS **TS-XVIIb** (Figure 6). In **XVIb**, the I−Li^1 distance is 3.781 Å, and the CH_3−I bond is not yet polarized (natural charge of 0.04 at I, and that of −0.02 at C^1H_3). In **TS-XVIIb**, the negative charge develops on the iodine atom (−0.29). In **TS-XVIb,** the Cu−C^a distance of 2.669 Å and the C^a−C^1 distance of 3.048 Å are longer than those in **TS-Vb**, and the X−C^1−H angles of 99° are larger than those of 94° in **TS-Vb**. These structural parameters indicate that the TS for CH_3I is earlier than that for CH_3Br. The activation energy of 14.9 kcal/mol is lower than that for the CH_3Br reaction as expected (cf. Figure 1b).

3. Kinetic Isotope Effects in the CH_3Br and CH_3I Reactions. Experimental primary and secondary KIEs at different temperatures have been determined[15] for the reaction of $(CH_3)_2CuLi{\cdot}LiCl{\cdot}PBu_3$ and CH_3I: 1.062 ± 0.003 (−17 °C) and 1.080 ± 0.002 (−60 °C) for the $^{12}CH_3I/^{13}CH_3I$ pair and 1.111 ± 0.006 (−16 °C) and 1.164 ± 0.004 (−63 °C) for the $CH_3I/C(^2H)_3I$ pair as shown in Table 1. These values imply linear symmetrical (as to the central carbon atom) and loose TS (as to the methyl hydrogen atoms).[53]

Theoretical KIEs[54] for the CH_3Br and CH_3I reactions were examined for the halide displacement stages and the Cu(III) reductive elimination stage in four different systems: the unsolvated, two solvent-coordinated and the doubly solvated models for $(CH_3)_2CuLi{\cdot}LiCl$, and the unsolvated model for $[(CH_3)_2CuLi]_2$. The results are shown in Table 1. Scanning of all theoretical data except **TS-VIIc** indicates that they are not much affected by either the nature of the leaving group solvation or the aggregation states of cuprates. In addition, data for the calculated KIEs for the **TS** of Cu(III) reductive elimination **TS-VIIc** (fourth row in Table 1) are quite different from those for the halide displacement. Comparison of the calculated and the experimental KIE data (bottom of Table 1) for the displacement step (all but **TS-VIIc**) and the reductive elimination steps (**TS-VIIc**) clearly indicates better concordance between theory and experiment for the displacement TSs, indicating that the halide displacement step is the rate determining step of the reaction. This conclusion naturally coincides with the computed energetics (Figure 1c) that the reductive elimination step via **TS-VIIc** is an extremely rapid step and hence cannot be the rate-determining step of the overall reaction.

Table 1. $^{12}C/^{13}C$ and $^1H/^2H$ KIE for $(CH_3)_2CuLi{\cdot}LiCl$ Reaction of Methyl Halides (B3LYP/631A) in the Reference of Reactants or a Precursor Complex **IVb** Used as a Computing Starting Material at Several Temperatures with Wigner Tunneling Corrections (Experimental Values for Methyl Iodide)

		$^{12}C/^{13}C$		H/D	
substrate		−17 °C	−60 °C	−16 °C	−63 °C
CH_3Br	**TS-Va**	1.069	1.082	1.167	1.209
	TS-Vb	1.074	1.088	1.178	1.226
	TS-Vc	1.071	1.084	1.158	1.197
	TS-VIIc	1.031	1.036	1.398	1.506
	TS-XIIIa	1.071	1.084	1.187	1.238
	TS-XIVb	1.073	1.087	1.156	1.199
CH_3I	**TS-XVIIb**	1.053	1.062	1.128	1.156
	TS-XVIIb[a]	1.053	1.062	1.172	1.219
	exptl[b]	1.062	1.080	1.111	1.164

[a] Complex **IVb** using as a computing starting material. [b] Data $(CH_3)_2CuLi{\cdot}LiCl{\cdot}PBu_3$ and CH_3I taken from ref 15.

4. S_N2 Reaction with Epoxides. (a) Courses of Reaction. The S_N2 reaction of cuprate with an epoxide is an important synthetic reaction.[1,2,55] We first modeled the reaction of ethylene oxide with $(CH_3)_2CuLi{\cdot}LiCl$, $[(CH_3)_2CuLi]_2$, $(CH_3)_2CuLi{\cdot}LiCl{\cdot}(CH_3)_2S$, and $(CH_3)_2CuLi{\cdot}LiCl{\cdot}(CH_3)_2O$ (data not shown).[10,11,56] The stereochemistry of the substitution product is known experimentally to be inversion at the carbon center of an epoxide in the reaction of the methyllithium with ethylene oxide. It was already shown theoretically that the inversion pathway is favored over the retention pathway. The course of reaction is investigated without (Scheme 2, path E) or with an explicit $(CH_3)_2S$ molecule on lithium (path F) or on copper (path G), and also with consideration of solvent polarity for path F. (Formula coding extends to that used for CH_3Br, i.e., **a** and **b** etc.). We first located the TS of the C^1−O bond cleavage (in the absence of solvent, **TS-XX**). Two intermediates (**XIX** and **XXI**) and the second TS (**TS-XXII**) are found by the IRC following and subsequent geometry optimization. Another possibility (**XXIIIg**) was also examined. The reaction scheme, energy profile, and the detailed structures of the representative stationary points for $(CH_3)_2CuLi{\cdot}LiCl$, $[(CH_3)_2CuLi]_2$ are shown in Scheme 2 and Figures 7 and 8.

(53) Isaacs, N. S. *Physical Organic Chemistry*; Longman Scientific & Technical: Essex, UK, 1987; Chapter 7.

(54) Cf.: Hu, W.-P.; Truhlar, D. G. *J. Am. Chem. Soc.* **1995**, *117*, 10726−10734.

(55) For example: Marino, J. P.; de la Pradilla, R. F.; Laborde, E. *J. Org. Chem.* **1987**, *52*, 4898−4913.

(56) $(CH_3)_2O$ was also investigated as a model solvent and gave almost identical results. Data with $(CH_3)_2S$ are shown in the present article, as $(CH_3)_2S$, which is often present in a cuprate mixture owing to the use of $CuBr{\cdot}(CH_3)_2S$, is sometimes suspected to act as more than just a solvent (which was found here not to be the case).

Scheme 2. Reaction Course of S_N2 Reaction of Ethylene Oxide (**XVIII**) with $(CH_3)_2CuLi{\cdot}LiCl$ (**I**) and $(CH_3)_2CuLi{\cdot}LiCl{\cdot}(CH_3)_2S$ (denoted as S)[a]

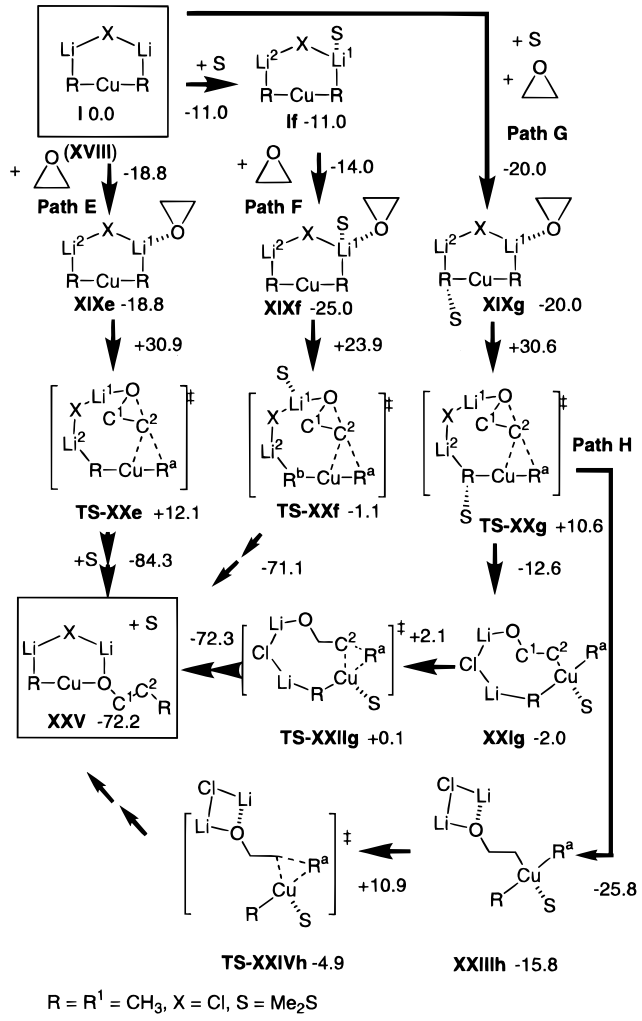

[a] The energy change on each step shown with an arrow is in kcal/mol. Minimum structures in the Path N (N = E, F, G, and H) are coded as roman numerals followed by n (n = e, f, g, and h, respectively) and written in bold. The energy change of each step shown with an arrow is in kcal/mol. Note that the final product mixture in the box is only formal, and the solvation or the change of aggregation states takes place in solution. Total energies of **I**, **XVIII**, and $(CH_3)_2S$ are −2195.576835, −153.786260, and −478.013808 hartrees at the B3LYP/631A level, respectively.

Reaction of dimeric cuprate, $[(CH_3)_2CuLi]_2$, is also examined (Figure 9). As was seen in the reaction of methyl bromide, the $O{-}C^2{-}C^aH_3{-}Cu{-}C^bH_3$ part structures of the precursor complex and the transition state are essentially the same. Activation energy of 29.2 kcal/mol in the $[(CH_3)_2CuLi]_2$ reaction is almost the same as that of 30.9 kcal/mol in the $(CH_3)_2CuLi{\cdot}LiCl$ case. Vibration modes are indicated by arrows.

The overall course of the reaction of ethylene oxide is found to be similar to that of the CH_3Br reaction except for the important stereochemistry of the electrophilic center C^2 (vide infra). A Lewis acid/base complex (**XIXe**) is formed first,[57] and then cluster opening takes place through cleavage of the electrostatic $Li^1{-}C^aH_3$ bond to reach the TS of $C^2{-}O$ bond cleavage (**TS-XXe**). This stage represents the rate-determining

(57) Harder, S.; Boersma, J.; Brandsma, L.; Kanters, J. A.; Duisenberg, A. J. M.; van Lenthe, J. H. *Organometallics* **1990**, *9*, 511−516.

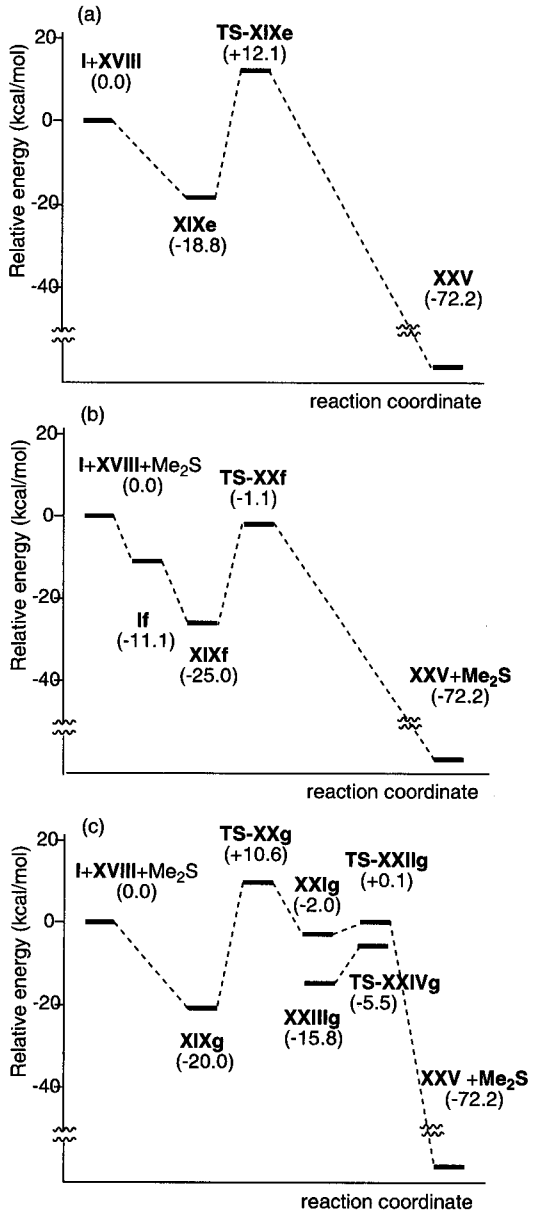

Figure 7. Energetics of the reaction of ethylene oxide with (a) $(CH_3)_2CuLi{\cdot}LiCl$ along path E, (b)$(CH_3)_2CuLi{\cdot}LiCl{\cdot}(CH_3)_2S$ along path F, and (c) $(CH_3)_2CuLi{\cdot}LiCl{\cdot}(CH_3)_2S$ along path G.

step of the overall reaction (Figure 7). In the absence of $(CH_3)_2S$, **TS-XXe** leads directly to the product (**XXV**) through $C^2{-}C^a$ bond formation. Placement of a solvent $(CH_3)_2S$ molecule in the vicinity of the copper atom (path G) modifies the reaction pathway, and the sulfide molecule becomes coordinated to the copper atom (**XXIg**) after the $C^2{-}O$ bond is mostly cleaved (i.e., the negative charge on cuprate is transferred to the oxygen atom). The Cu(III) intermediate **XXIg** undergoes reductive elimination with a very small activation energy (**2.1** kcal/mol) to form the product complex (e.g., **XXV**).[8]

The transition structure (**TS-XXe**) of the C−O displacement with $(CH_3)_2CuLi{\cdot}LiCl$ is shown in Figure 8. We find in **TS-XXe** that the lithium cuprate cluster is opened and the epoxide $C^2{-}O$ bond is breaking due to the push−pull action of the open cluster. Such push−pull activation is also observed in the reaction with CH_3Br as well as in the addition reactions of lithium organocuprates(I). Owing to the directionality of the epoxide lone pair, the $C^a{-}Cu{-}C^b$ bond approaches the epoxide in a manner nearly orthogonal to the $C^1{-}C^2{-}O$ epoxide plane

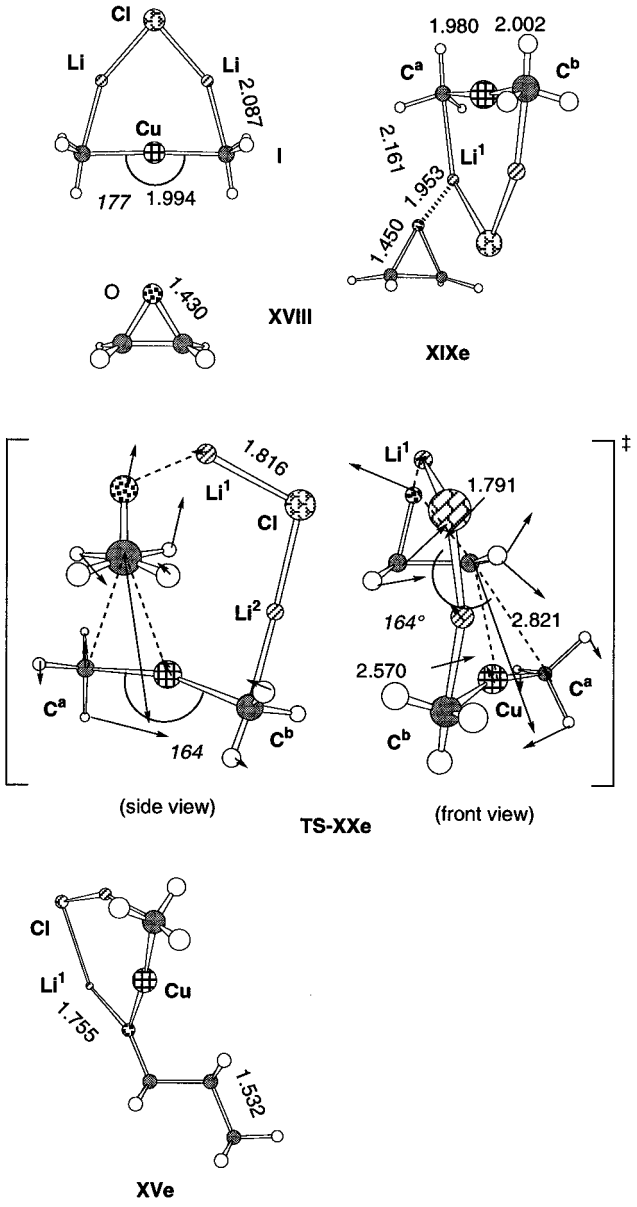

Figure 8. B3LYP stationary points in the reaction of $(CH_3)_2CuLi\cdot LiCl$ with ethylene oxide. Bond lengths in Å, bond angles (in italic) in deg, and natural charge (in underlined bold) are given. The value of an imaginary frequency in **TS-XXe** is 410.1*i* cm^{-1}.

as seen in the front view of **TS-XXe**. The C^2-O bond in **TS-XXe** is elongated by 25% (1.79 Å) relative to ethylene oxide (1.43 Å) and the stereochemistry of the C^1 atom is already inverted. Thus, the TS of the epoxide reaction is more advanced than that of the CH_3Br substitution reaction (18% elongation of the C−Br bond with the stereochemistry yet to inverted vide supra). The more advanced transition state for the epoxide reaction is the result of the release of the ring strain at an earlier possible stage of the reaction. Strain effects moving the position of transition state earlier on the potential surface are discussed in detail for the reaction of cyclopropene.[58]

Solvent coordination and solvent polarity affect the activation energy. The gas-phase activation energy from the very stable Li^1-O complex (**XIXe**) to **TS-XXe** (path E) is as much as 30.9 kcal/mol (B3LYP/631A, Figure 9). When the $(CH_3)_2S$ is coordinated to Li^1 (path F, **XIXf** to **TS-XXf**), the Lewis acidity

(58) Nakamura, E.; Nakamura, M.; Miyachi, Y.; Koga, N.; Morokuma, K. *J. Am. Chem. Soc.* **1993**, *115*, 99−106.

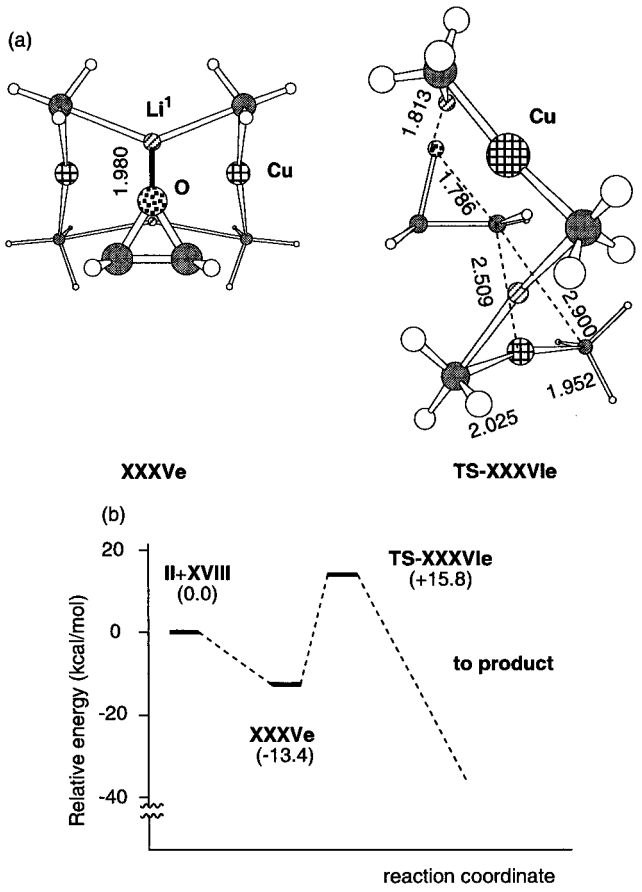

Figure 9. (a) B3LYP stationary points in the reaction of $[(CH_3)_2CuLi]_2$ with ethylene oxide. Bond lengths in Å, bond angles (in italic) in deg, and natural charge (in underlined bold) are given. A value of an imaginary frequency in **TS-XXVIe** is 409.4*i* cm^{-1}. (b) Energetics of the reaction with ethylene oxide.

of Li^1 is attenuated and the activation energy decreases to 23.9 kcal/mol. When the solvent polarity ($\epsilon_0 = 4.3$ for ether, 20 °C) was considered with the polarized continuum model (PCM) for path E (no explicit solvent), the activation energy is 24.1 kcal/mol (B3LYP(PCM)/631A//B3LYP/631A). Therefore, we expect a ca. 20kcal/mol activation energy in solution.

While solvent coordination to Cu does not take place before the C−O cleavage (**TS-XXg**, Figure 11),[31] it does occur after **TS-XXg** and significantly changes the course of the reaction (the same was found for CH_3Br, vide supra). Thus, when a $(CH_3)_2S$ molecule is placed near the copper atom in **TS-XXe** and the reaction pathway is followed along the IRC, $(CH_3)_2S$ becomes strongly attached to the copper atom as the C^1-O bond cleavage is advanced.

This transformation accompanied the formation of an alkoxide anion and a Cu(III) center to give an intermediate (**XXIg** or **XXIIIh**) in Figure 11. IRC analysis does not connect directly from **TS-XXg** to **XXIIIh**, in which two lithium atoms bond to an epoxy oxygen, but the formation of **XXIIIh** is quite likely in solution. This Cu(III) intermediate is kinetically unstable, and undergoes C−C bond forming reductive elimination through the second TS (**TS-XXIIg** or **TS-XXIVh**, Figure 11) to give the product, propanolate anion incorporated in a new cluster (Scheme 2; **XXV**, which represents only one example of a number of conceivable product structures).

(b) BF_3 Effects. Nucleophilic ring opening of epoxide is accelerated in the presence of BF_3. To examine how this acceleration occurs, we focused on several important stationary points in the above reaction pathways, and allowed BF_3 to

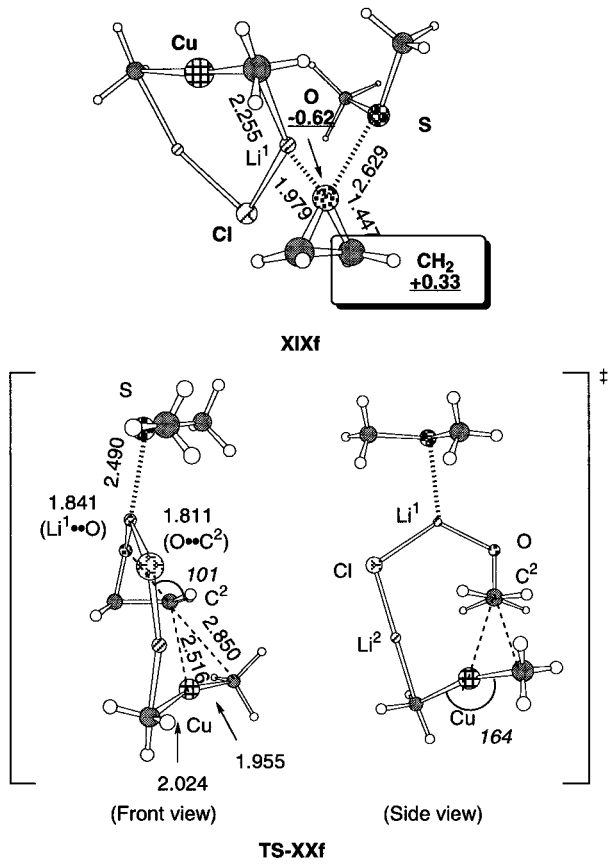

Figure 10. 3D structures of **XIXf**, and **TS-XXf** at the B3LYP/631A level. The value of an imaginary frequency for **TS-XXf** is 320.9*i* cm^{-1}.

coordinate to the epoxide oxygen atom of these structures (Scheme 3). 3D structures of the stationary points are shown in Figure 12. For comparison, path F, which is already depicted in Scheme 2, is shown again in Scheme 3.

The coordination of BF_3 to a cuprate gives a complex **XXVII** in which a fluorine atom of BF_3 is coordinated to two lithium atoms of cuprate. A nearly linear arrangement of the C−Cu−C moiety (170°) indicates there may be a small interaction between B and Cu atoms. Alternatively, by putting first BF_3 on the epoxide, the epoxide/BF_3 complex **XXVI** forms. The energy of BF_3 + **If** + **XXVI** is 1.7 kcal/mol more stable than that of epoxide + **XXVII**, and 1.8 kcal/mol less stable than **XIXf** + BF_3 in which both $(CH_3)_2S$ and an epoxide oxygen are coordinated to Li^1. Coordination of a fluorine atom of **XXVI** to Li^1 of **If** generates the structure **XXVIIIi** with 13.1 kcal/mol exothermicity, and coordination of an oxygen atom of **XXVI** to Li^1 of **If** affords the structure **XXIX** with 15.8 kcal/mol exothermicity.[59] From **XXXVIIIi**, we easily reached the transition state of the BF_3-assisted C−O bond cleavage **TS-XXXi**. Here the epoxide oxygen interacts strongly with the boron atom as shown in Figure 12.

3D structures are shown in Figure 12. Notably, the shrinking Li^1••O distance of 2.67 Å is shorter than that of 3.70 Å in **XXVIIIi**, but is longer than that of 1.84 Å in **TS-XXf** in the absence of BF_3. In **TS-XXXi**, there is an interaction between Li^1 and F. The Li^1••F distance in **TS-XXXIi**, 1.83 Å, is shorter than that of **XXVIIIi**, 1.92 Å. The distance of the breaking C^2−O bond in **TS-XXXIi** is shorter than that of 1.81 Å in **TS-XXf**, indicating that the transition state in the presence of BF_3 has a more product-like character than the transition state in the absence of BF_3.

Scheme 3. Reaction Course of S_N2 Reaction of Ethylene Oxide (**XVIII**) with $(CH_3)_2CuLi{\cdot}LiCl{\cdot}(CH_3)_2S$ (denoted as S) with BF_3[a]

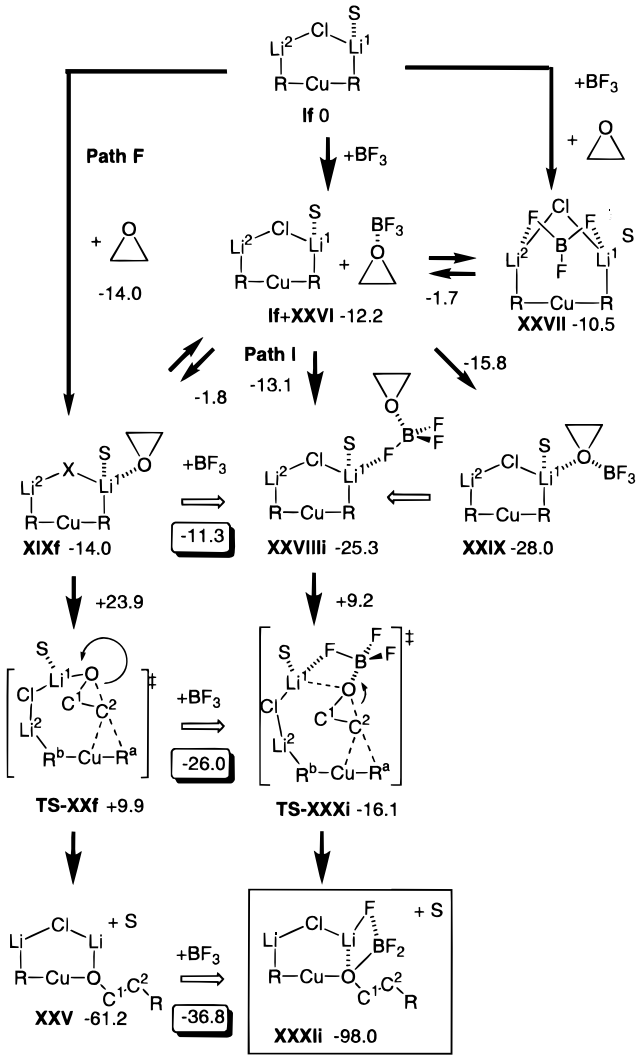

[a] The energy change of each step shown with an arrow is in kcal/mol. Energetics of each step shown with an arrows is in kcal/mol. Note that the final product mixture in the box is only formal, and actually solvation or the change of aggregation states in solution takes place. Total energy of BF_3 is −324.5532420 hartree at the B3LYP/631A level.

When we compare the energetics of path F, **XIXf** → **TS-XXf** → **XXV**, with that of the path **XXVIIIi** → **TS-XXXi** → **XXXIi** (hollow arrows in Scheme 3), it becomes clear that BF_3 stabilizes the TS and the product more than the starting material: The stabilization energies resulting from the coordination of BF_3 are 11.3, 26.0, and 36.8 kcal/mol in the precursor complex, the transition state, and the product, respectively. Such stabilization effect is caused by the strength of the B••O interaction.

In summary, BF_3 acts as an effective Lewis acid on the starting epoxide through two points binding (B−O and O−Li−F) to the cuprate/epoxide complex. A similar mode of action of BF_3 on an electrophile may also be operating in the starting material activation in the BF_3-accelerated conjugate addition (cf. ref 22e).

(c) Cyclohexene Oxide: Trans-Diaxial Ring Opening. Despite many similarities between the transition structures of

(59) (a) Hine, J.; Linden, S.-M.; Kanagasabapathy, V. M. *J. Am. Chem. Soc.* **1985**, *107*, 1082−1083. (b) Asao, N.; Kii, S.; Hanagawa, H.; Maruoka, K. *Tetrahedron Lett.* **1998**, *39*, 3729−3732. (c) Omoto, K.; Fujimoto, H. *J. Org. Chem.* **2000**, *65*, 2464−2471.

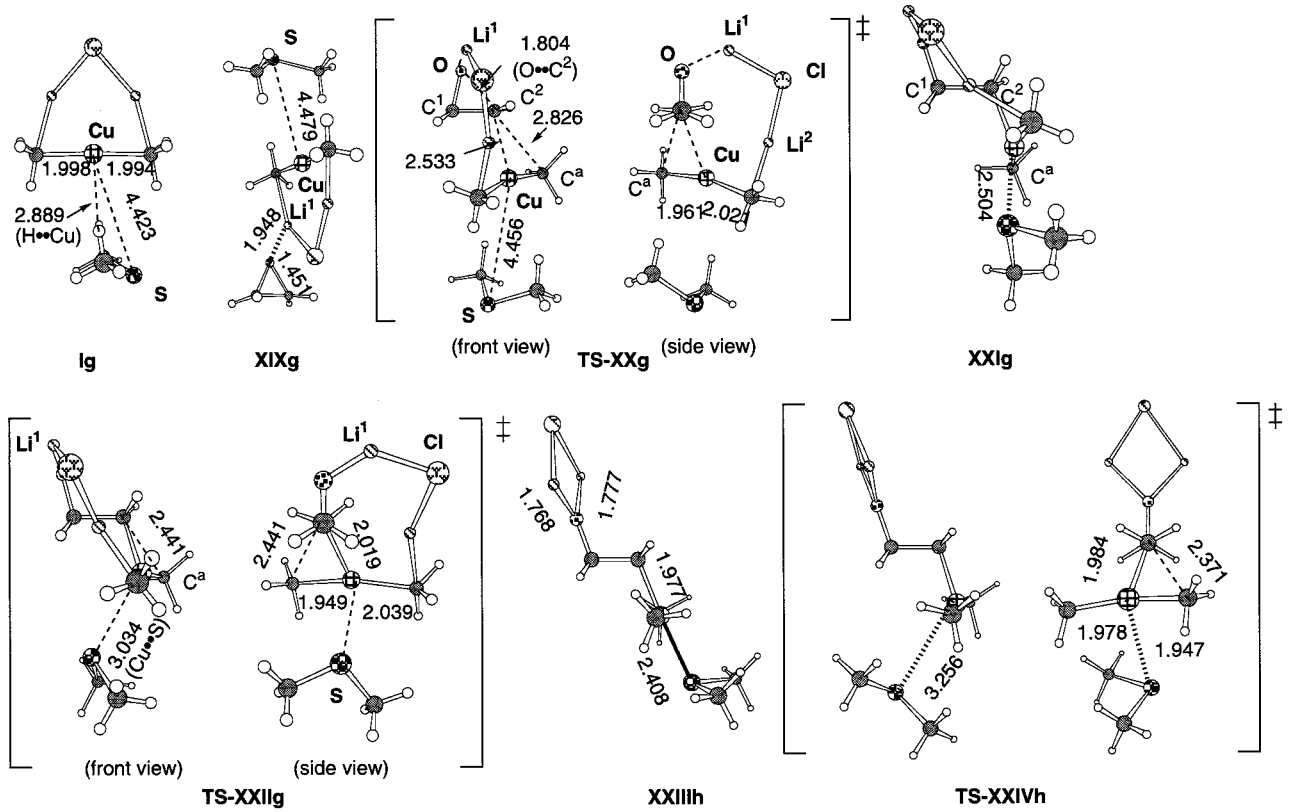

Figure 11. B3LYP stationary points in the reaction of $(CH_3)_2CuLi{\cdot}LiCl{\cdot}(CH_3)_2S$ with ethylene oxide. See Figure 2 for details. The values of imaginary frequencies for **TS-XXIIg** and **TS-XXIVh** are 73.4*i* and 151.0*i* cm^{-1}, respectively.

the CH_3X reaction and the epoxide reaction, they differ in one important point, that is, the stereochemistry of the electrophilic carbon center is inverted in the latter, not in the former. We found that the inverted stereochemistry can be related to the trans-diaxial ring opening in the reaction of cyclohexene oxide (cf. eq 2).

Let us take the example shown in eq 2. If the cuprate attacks the 4-position (relative to R^1) with inversion, it will attack the epoxide from the axial direction giving **3**. If the attack occurs on the 3-position, the nucleophilic R group becomes attached to the equatorial position as in **5**. We studied the TSs structures of these two pathways for the most realistic model of the system, namely, cyclohexene oxide itself.

As shown in Figure 13, we found that the TS corresponding to the trans-diaxial opening has the chair structure **TS-XXXII**, and the TS leading to the diequatorial opening product **5** has the twist-boat structure **TS-XXXIII**. Cleaving C^1-O distances of 1.955 and 1.993 Å are larger than that of 1.791 Å in the ethylene oxide reaction (**TS-XXe**, Figure 8). The trans-diaxial opening transition state is favored over the alternative by 3.5 kcal/mol (3.6 kcal/mol with correction of zero-point energy; $\Delta\Delta G^{\ddagger} = 3.8$ kcal/mol at 298.15 K). When we removed the cuprate moiety from these two TSs (Figure 13c,d), the energy difference of the isomeric cyclohexene oxide core structures became 5.4 kcal/mol.[60] This value indicates that the energy difference of 3.5 kcal/mol between the diaxial and the diequatorial openings largely arises from the conformational effects of the six-membered carbocycle. The fundamental reason for the diaxial opening is therefore the inverted stereochemistry of the electrophilic center that arises in turn from the ring strain of the epoxide ring.

(60) Energies of these fragments are calculated for singlet, and triplet energies are about 48 kcal/mol higher than those for singlet.

5. Orbital Interactions Responsible for the S_N2 Reactions. As mentioned in section C.1, the most important structural feature of all the TS of the displacement stage is that the C^a-Cu-C^b geometry is nearly linear. This geometry stands in contrast to the bent geometry found in the additions of cuprates to acetylene and olefin. To learn what orbitals are responsible for the S_N2 reaction with retention of the linear geometry, we examine the localized molecular orbitals (LMOs) of the TSs of CH_3Br and ethylene oxide reactions. The C−Cu LMOs of **TS-Va** (the CH_3Br reaction) and **TS-XXe** (the ethylene oxide reaction) shown in Figure 14 indicate that the C−Cu σ-bond composed of copper $3d_{z^2}$ and the methyl 2s/2p orbitals interact with the C−X σ^*-bond orbital. We have reported a rationalization of the linear C^a-Cu-C^b geometry in the light of HOMO of $(CH_3)_2Cu^-$.[22d]

6. Conclusion and Implications in Organic Chemistry. The present study represents the first theoretical analysis of the reactivities of organocuprate(I) clusters with sp^3-alkylating agents. Two representative classes of alkylating agents, alkyl halides and epoxides, have been examined for typical cuprate cluster reagents in the presence of solvents ($(CH_3)_2O$ and $(CH_3)_2S$) that have affinity toward both lithium and copper. We have probed the role of BF_3 that is widely used to promote the reaction of lithium cuprates with epoxide. The usefulness of the chemical and theoretical models as a probe of solution chemistry of cuprate clusters in question was supported by the studies on KIE and on the trans-diaxial regioselectivity of cyclohexene oxide opening. It must be noted that the same chemical models $(CH_3)_2CuLi{\cdot}LiCl$ and $[(CH_3)_2CuLi]_2$ have successfully been employed as useful models of the solution chemistry of the conjugate addition of cuprate.[22,61]

Stereochemistry by theory is consistent with the experimental stereochemistry by showing that the net result of the SN2

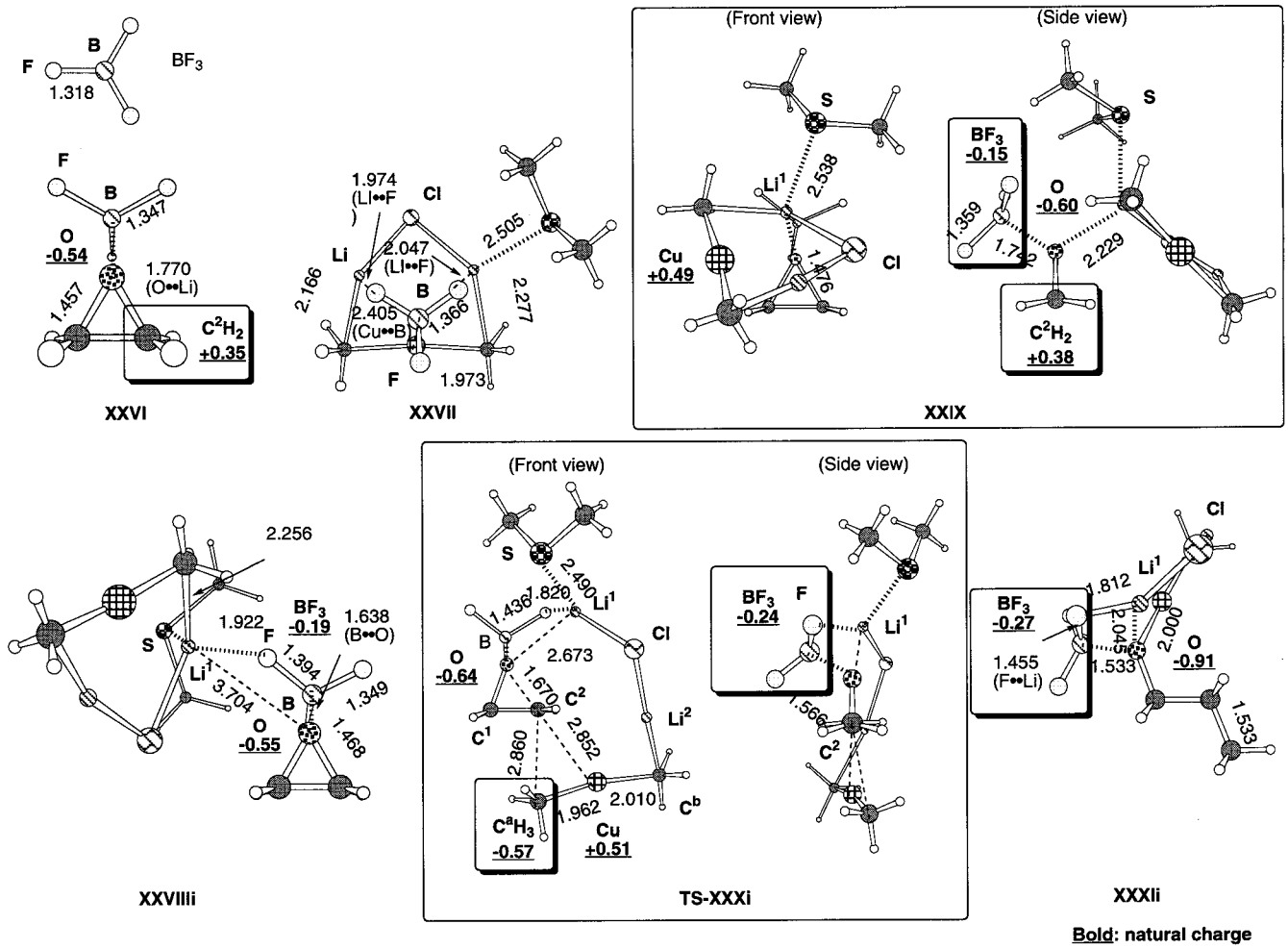

Figure 12. 3D structures of stationary points in the reaction of $(CH_3)_2CuLi{\cdot}LiCl{\cdot}(CH_3)_2S{\cdot}BF_3$ with ethylene oxide at the B3LYP/631A level. See Figure 2 for details. The value of an imaginary frequency for **TS-XXVI** is 320.9 cm^{-1}.

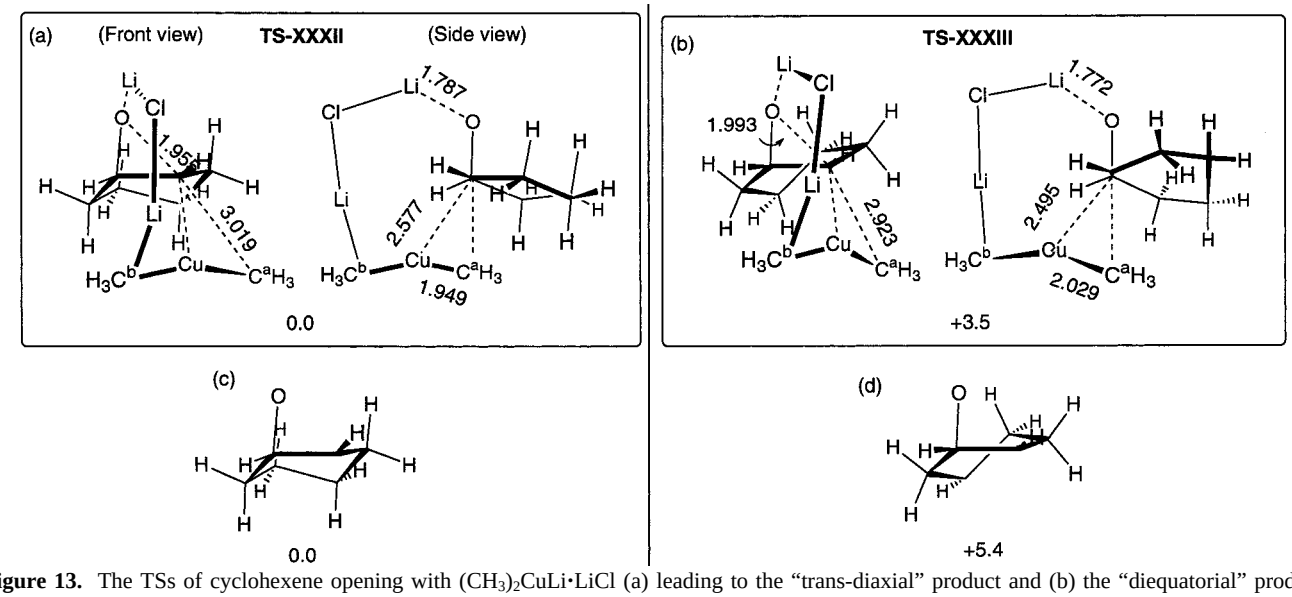

Figure 13. The TSs of cyclohexene opening with $(CH_3)_2CuLi{\cdot}LiCl$ (a) leading to the "trans-diaxial" product and (b) the "diequatorial" product (UB3LYP/631A//B3LYP/631A) and (c, d) the epoxide position of the TS devoid of the cuprate cluster and their relative energies in kcal/mol.

reaction through all paths A−D is inversion at the electrophilic carbon center and retention at the nucleophilic carbon center. The rate-determining step of the S_N2 alkylation reaction of alkyl halide and epoxide has been shown to be the substitution step rather than the reductive elimination step of the intermediary copper(III) intermediate, whose structure provided a convincing reason for the long standing question about the selective formation of a heterocoupling product $R-R^1$ in the reaction of R_2CuLi and R^1X (eq 5).

(61) The behavior of organocuprate aggregates in solution was recently discussed in a review. See: Nakamura, E.; Mori, S. *Angew. Chem.* Accepted for publication.

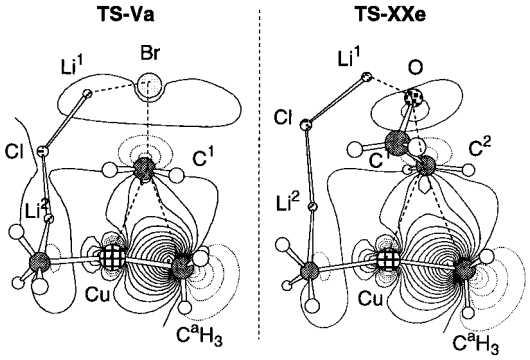

Figure 14. Localized Kohn−Sham orbitals in **TS-Va** of the CH_3Br reaction left and in **TS-XXe** of the epoxide reaction right are shown in the C^1−Ca−Cu plane, with the contours from −0.25 to +0.35 at intervals of 0.025 in e•au^{-3}, with positive and zero contours in solid and negative in dotted curves.

We have previously shown for the addition reactions (i.e., carbocupration of acetylene and conjugate addition reactions)[22a,b] that the two lithium cuprate clusters, R_2CuLi dimer **A** and R_2-CuLi•LiCl complex **B**, have a large enough cluster size to achieve synergetic electron flow within a cluster/electrophile complex, allowing the lithium atom(s) to activate the electrophile, to which the copper(I) (through its $3d_{xz}$ orbital) pumps electrons to the π*-orbital. In this way, the rather stable carbon-Cu(I) bond weakens by forming a organocopper(III) species so that facile transfer of the R group from copper to the electrophile takes place readily.

In the present study, we have identified two major differences between the S_N2 alkylation reaction and the addition reactions. The first difference resides in the use of the copper s + $3d_{z^2}$ orbital in the alkylation reaction (rather than $3d_{xz}$ in the additions),[22a,b] since the key orbital interactions involve the σ* orbital of the alkylation agent (rather than the π* orbital). As is seen in the LMOs shown in Figure 14, the TS of the displacement may be viewed both as a nucleophilic reaction of the copper atom and as that of the methyl anion. Therefore, the mechanistic reality of the S_N2 reaction resides halfway between the two existing mechanistic proposals discussed in eqs 4 and 5.

The second difference is the rate- and stereochemistry-determining step of the reaction. In the alkylation reaction, this step is the displacement step leading to the Cu(III) intermediate. The resulting trialkylcopper(III) intermediate (**VIc** or **VIIId**) decomposes quickly in the alkylation reaction. In the conjugate addition (eq 6), the copper(III) intermediate is stable and its

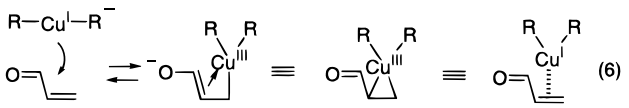

reductive elimination becomes the rate- and stereochemistry-determining step, because the copper(III) center here possesses a strong internal donor ligand (i.e., enolate) which decelerates the reductive elimination. In this regard, this copper(III) intermediate is essentially the same as the species generally regarded either as a cuprio(III)cyclopropane or as an olefin/Cu(I) π-complex.

A plausible mechanism of S_N2 alkylation of the $(CH_3)_2CuLi$•LiX cluster (X = halide, alkoxide, R_2Cu^-) in ethereal solution is shown in Scheme 4 (solvent molecules on lithium are omitted). The cluster (**A** or **B**) traps the alkylating agent RY

Scheme 4

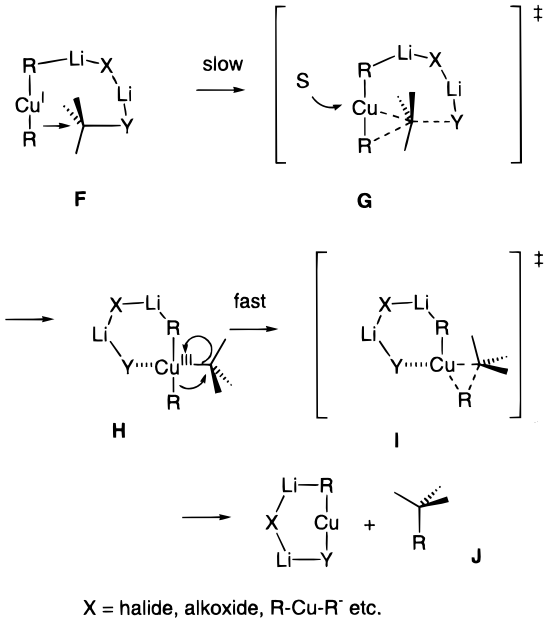

Scheme 5

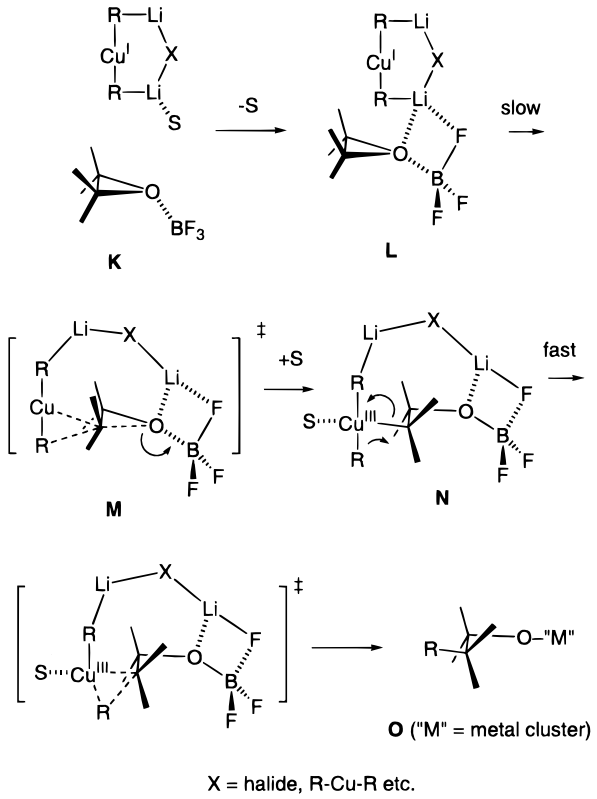

and the resulting open cluster **F** leads to the TS of displacement (**G**) with retention of the linear R_2Cu^- geometry. After displacement, a kinetically unstable Cu(III) complex **H** forms.[22f] The geometry of such a complex is such that the homocoupling of the two R groups is prohibited. The reductive elimination step **I** takes place with retention of the stereochemistry of the carbon centers to give the cross coupling product **J**. One can further speculate participation of an additional lithium halide atom acting as a Lewis acid as discussed below for BF_3 activation.

A plausible pathway of the BF_3 participation in the epoxide opening is shown in Scheme 5. An epoxide/BF_3 complex **K**

may encounter the cuprate cluster to form a ternary complex **L** or such a complex may form also from a cuprate/BF_3 complex and the epoxide. The displacement TS (**M**) followed by the formation of a Cu(III) intermediate (**N**) gives the alkylation product **O**. We may also speculate that excess lithium halide present in the cuprate reactions may play a role similar to BF_3 but to a lesser extent. Note that the coordination of BF_3 on a Cu(III) intermediate, which we recently suggested was important in the conjugate addition reaction,[22f] may likely be unimportant since the Cu(III) intermediate **N** is not a rate-determining step in the epoxide reaction.

The TSs of cyclohexene oxide (Figure 13) provided the first theoretical explanation for the trans-diaxial regiochemistry of cyclohexene oxide ring opening. The selectivity originates from the preferred chair transition state **TS-XXVI**. This preference originates from the inverted stereochemistry of the electrophilic carbon atom, which, in turn, originates from the stretching of the C−O bond caused by the epoxide ring strain (vide supra). The argument based on the chair/twist-boat transition state is an old one, but the present study offered the first theoretical background and the molecular geometries for this important synthetic process.

In summary, the present study provides a detailed mechanistic pathway for the transition metal mediated alkyl−alkyl coupling reaction. The S_N2 displacement process starting with R^1−Y to go eventually to R^1−R through the R^1−Cu−Y complex (**VIIId**) (Scheme 1) represents a typical oxidative addition/reductive elimination reaction involving an organic halide, and will serve as a useful model for this important yet mechanistically obscure sequence in the transition metal chemistry.[62]

Acknowledgment. This work was supported by Monbusho Grant-in-Aid for Scientific Research on Priority Area (No. 283) and by a grant from the U.S. National Science Foundation (CHE-9627775). E.N. and K.M. are grateful for a JSPS-NSF Joint collaborative research award (INT-9726789). Generous allotment of computational time from the Institute for Molecular Science, Okazaki, Japan, and the National Center for Supercomputing Applications, Illinois, is deeply acknowledged. S.M. is grateful for a JSPS research fellowship.

Supporting Information Available: Geometries of the representative stationary points (PDF). This material is available free of charge via the Internet at http://pubs.acs.org.

JA0002060

(62) 3D pictures and coordinates of the structures in this paper are available at the following: http://WWW.chem.s.u-tokyo.ac.jp/~common/Theo/Sn2/title.